CHAPTER IV

RESULTS AND DISCUSSION

4.1 Characterization of LDPE and LLDPE

Typical DSC thermograms of LDPE and LLDPE are shown in Figure 4.1. T_m of LDPE and LLDPE was at 101.1 and 119.9°C, respectively. T_c of LDPE and LLDPE was at 95.2 and 111.2°C, respectively. The percentage of crystallinity of LDPE and LLDPE was determined to be 31.1 and 34.9%, respectively.
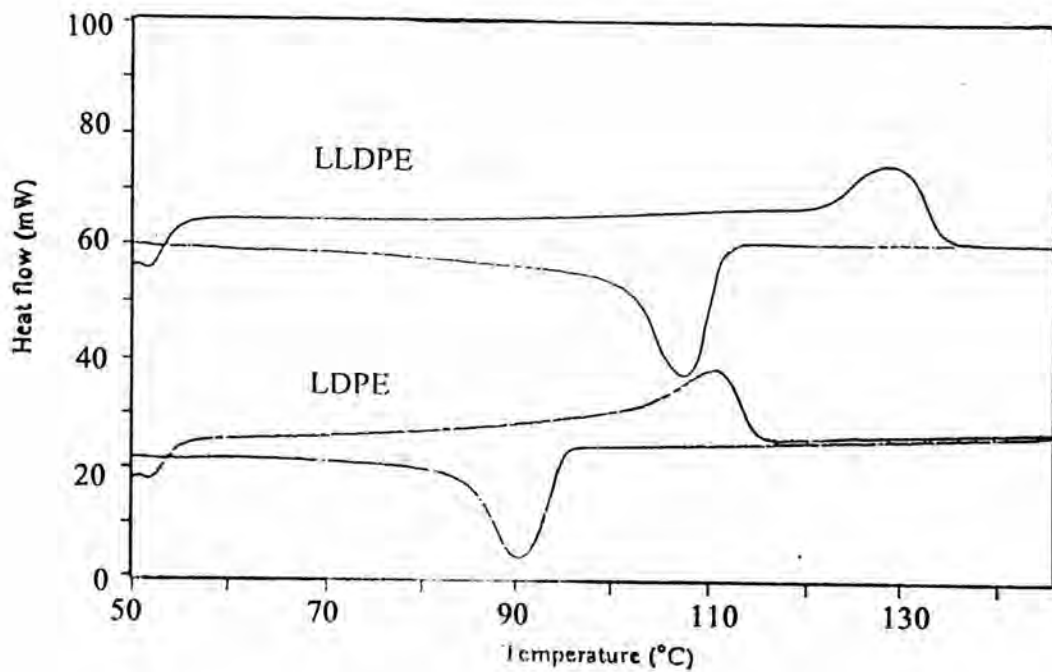

Figure 4.1 The DSC thermograms of LDPE J4324 and LLDPE L2020F.

Heat of fusion of LDPE and LLDPE are equal to 21.3 and 23.9 cal/g, respectively.
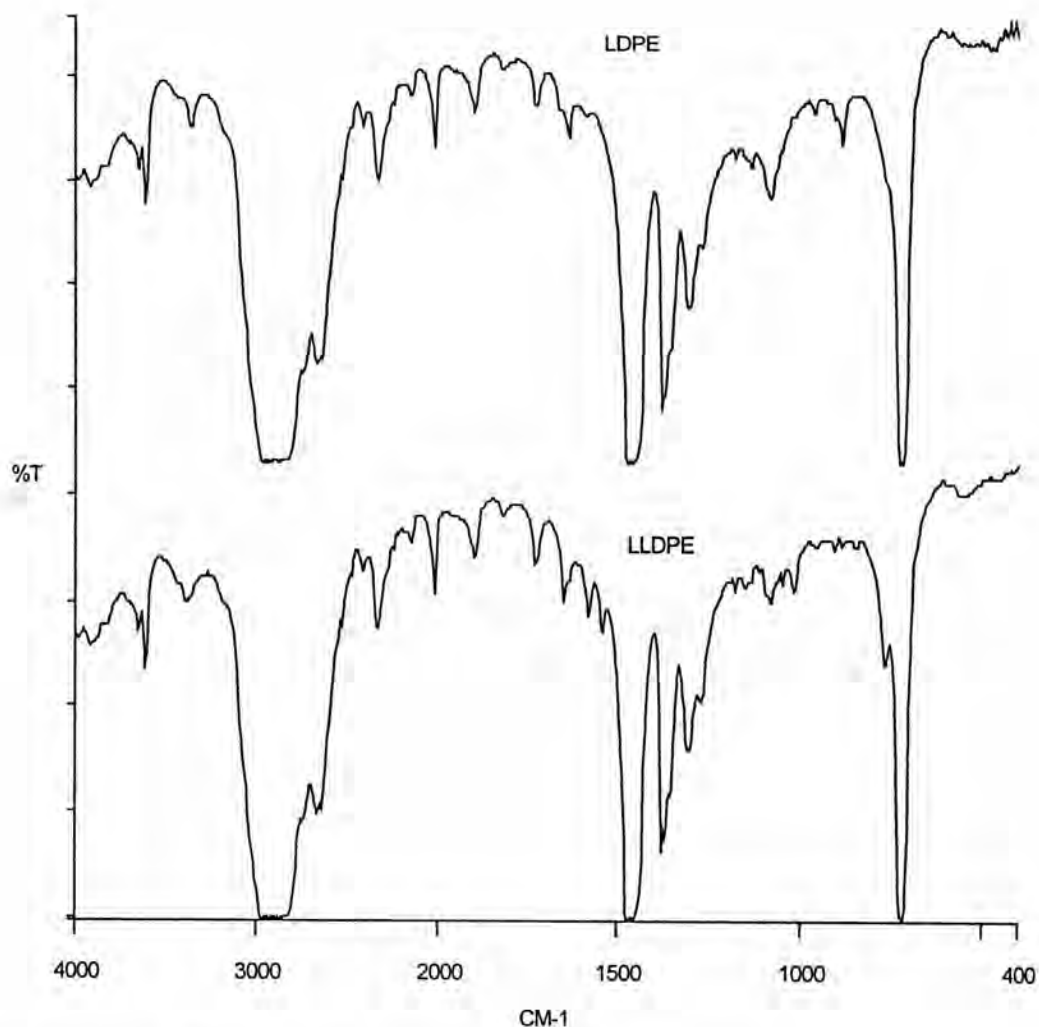
Figure 4.2 FT-IR spectra of LDPE J4324 and LLDPE L2020 F.

The IR spectra of LDPE and LLDPE are show in Figure 4.2. Only the methyl rocking band ranging from 680 to 780 cm^{-1} of LLDPE was found to be different from LDPE.

The melt flow index (2.16 kg load at 190°C) of LDPE and LLDPE was respectively 2.01 and 1.89 g/10 min. This implied that MW of LLDPE was slightly higher than that of LDPE, which was supported by the measured M_w values of LDPE and LLDPE by GPC technique to be 228,127 and 232,405 g/mol, respectively. The polydispersity index of LDPE and LLDPE was of 9.2 and 8.7, respectively.

4.2 Determination of Short Chain Branching of Polyethylene

The number of short chain branching of LDPE and LLDPE was determined by the FT-IR technique, and the method was described by Usami and Takayama [18]. Differences of intensities of the band at 1378 cm^{-1} (assigned as the methyl symmetrical deformation band near 1378 cm^{-1}) of the branch polyethylene (LDPE and LLDPE) from that of high density polyethylene (HDPE) were used for the calculation of branch concentration.

$$N = (K \cdot A)/ (T \cdot D) \tag{4.1}$$

where N = branch concentration per 1000 carbon atoms

K = absorption coefficient having the value of 0.039

A = absorbance

T = thickness of sample film, cm

D = film density, g/cm^3.

Typical IR spectra of LDPE, LLDPE and HDPE in the regions of 1300-1400 cm^{-1} are shown in Figure 4.3 a-c. The subtracted spectra of LDPE and LLDPE with HDPE in those region are also shown in Figure 4.3 d-e. The methyl group per 1000 carbon atoms of LDPE and LLDPE was calculated to be 1.66 and 1.43, respectively. The experimental data are given in Appendix A. The number of short chain branching of LDPE was a little bit higher than that of LLDPE so that the crystallinity and melting temperature of the former were lower than the latter.
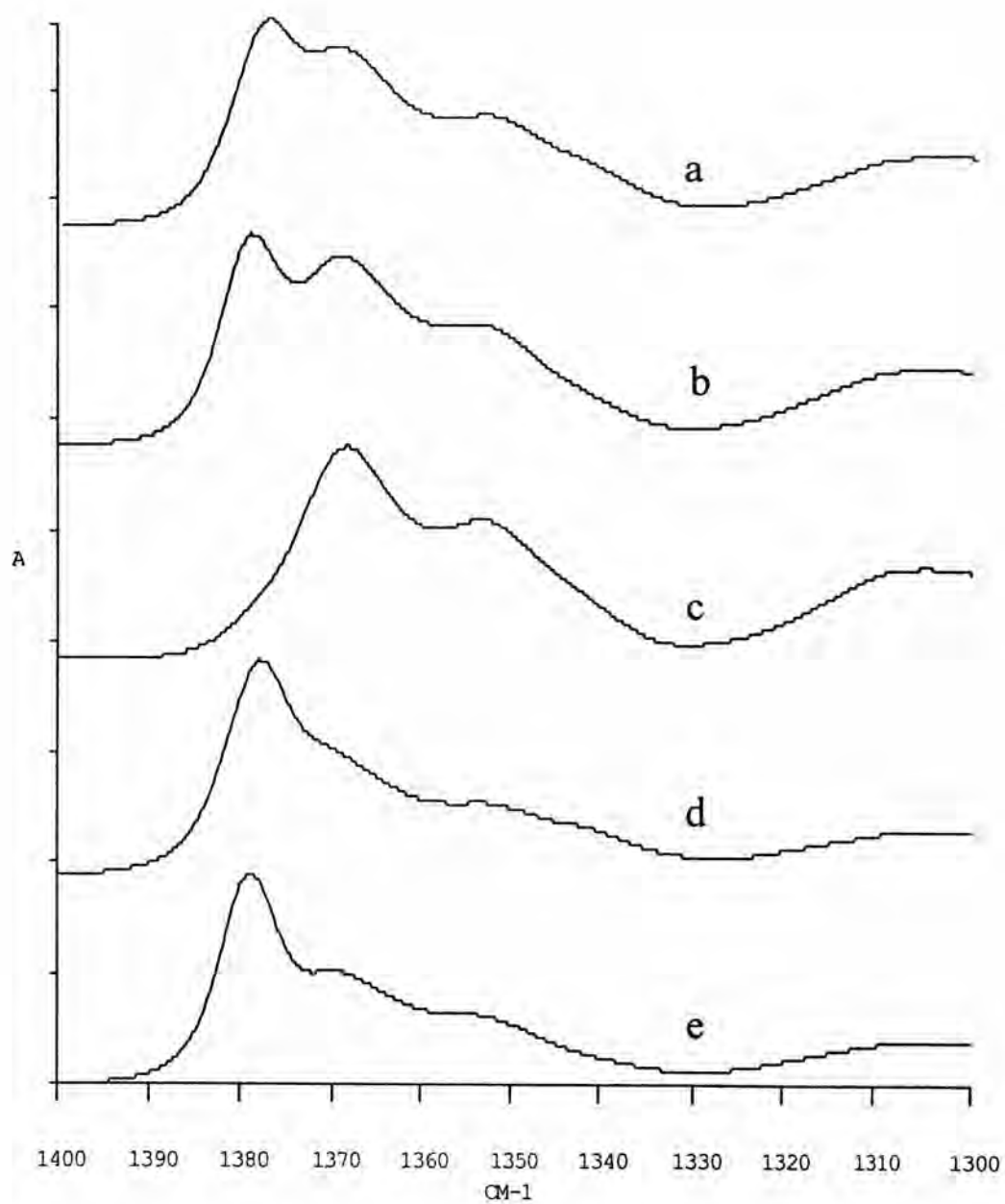
Figure 4.3 FT-IR spectra of the methyl symmetrical deformation band at 1300–1400 cm^{-1} of (a) LDPE, (b) LLDPE, (c) HDPE, (d) subtraction band of LDPE from HDPE, and (e) subtraction band of LLDPE from HDPE.

4.3 Kinetics Study of Peroxide Crosslinking Reaction of LDPE and LLDPE Using Rheometric and Differential Scanning Calorimetric Techniques

The kinetics of crosslinking reactions of LDPE and LLDPE in the presence and in the absence of an inhibitor were studied by using both rheometric and differential scanning calorimetric techniques. The former technique, PL 2000 Brabender Plasti-Corder (BPC) was used and the latter technique, differential scanning calorimeter (DSC) was employed. The mixing chamber of BPC and aluminium pans of DSC were used as reactors. There was a twin contra-rotating screw in the BPC chamber, the rotor speed was controlled at 50 rpm, so that the polymer material was subjected to the mechanical shear force. For the DSC technique, no external forces was applied to the polymer system. Results of the kinetic study obtained from both techniques render the significant details understanding of the kinetics. The terms "RHE" and "DSC" appeared hereafter refer to the rheometric and DSC techniques, respectively.

4.3.1 Kinetics of Crosslinking Reaction in the Absence of an Inhibitor

Figures 4.4 and 4.5 show the plots of torque and temperature of materials in the mixing chamber against time of the crosslinking reactions of LDPE and LLDPE at 446 K at various DCP concentrations ranging from 0 to 2.4%w/w and in the absence of Irganox 1010. The maximum torque increased with increasing DCP loading from 0 to 1.2% by weight and reached the maxima at DCP concentration (see Figure 4.6). In the other words, it implied that the crosslinking reaction of polymers increased when the DCP concentration increased from 0 to 1.2% for LDPE and 0 to 1.0% for LLDPE, respectively. The excess amount of DCP in the reaction should result in increases of the number of crosslinks in the interchain of the crosslinked polymer, i.e., the increase of the crosslink density. After the maxima, the torques decayed when the crosslinked polymers were sheared in a long period of time because they degraded by the chain scission. The decline of LDPE torques was found more rapid than those of LLDPE because the LDPE degraded easier due to the existing of longer chain branching.

When they have been crosslinked, the longer chain branching in LDPE led to more free volume than LLDPE resulting in easy to oxidation or degradation.

After DCP loading, the melt temperature of the materials in the chamber increased proportional to conversion of the crosslinking reaction from zero to 98% after which it remained constant (see Figure 4.7). This indicated that the crosslinking reactions proceeded non-isothermally. The increase of temperature was of two folds including (a) due to the exothermic heat of the crosslinking reaction, and (b) due to the heat generation by the mechanical shear of the crosslinked polymers. Hence the temperature-time data was not utilized to determine the kinetic parameter, but the torque-time relationship was used instead. The maximum torques of LDPE and LLDPE (see Figures 4.4 and 4.5) were found at 29.6 and 56.0 Nm, respectively. The experimental data are given in Appendix B.

For the DSC technique, the kinetic parameters were determined from the relationships of heat flow versus temperature or time. Typical DSC thermograms (temperature scanning mode) of the crosslinking reaction of LDPE and LLDPE are shown in Figures 4.8 and 4.9. Table 4.1 shows the total heat of reaction of LDPE and LLDPE at various DCP concentrations. It can be seen that the amount of DCP increased, the number of alkoxy radicals also increased leading to the increase of total heat of reactions.

The method to determine the crosslinking conversion at particular time was described in Sections 3.4.1 and 3.4.2 for the rheometric and DSC techniques, respectively. The plots of crosslinking conversion (x) versus reaction time (t) of the crosslinking reactions of LDPE and LLDPE in the absence of Irganox 1010 at various DCP concentrations are shown in Figures 4.10-4.11 for Rheometric technique and 4.12-4.13 for DSC technique. The detail of all data are shown in Appendix B-E.
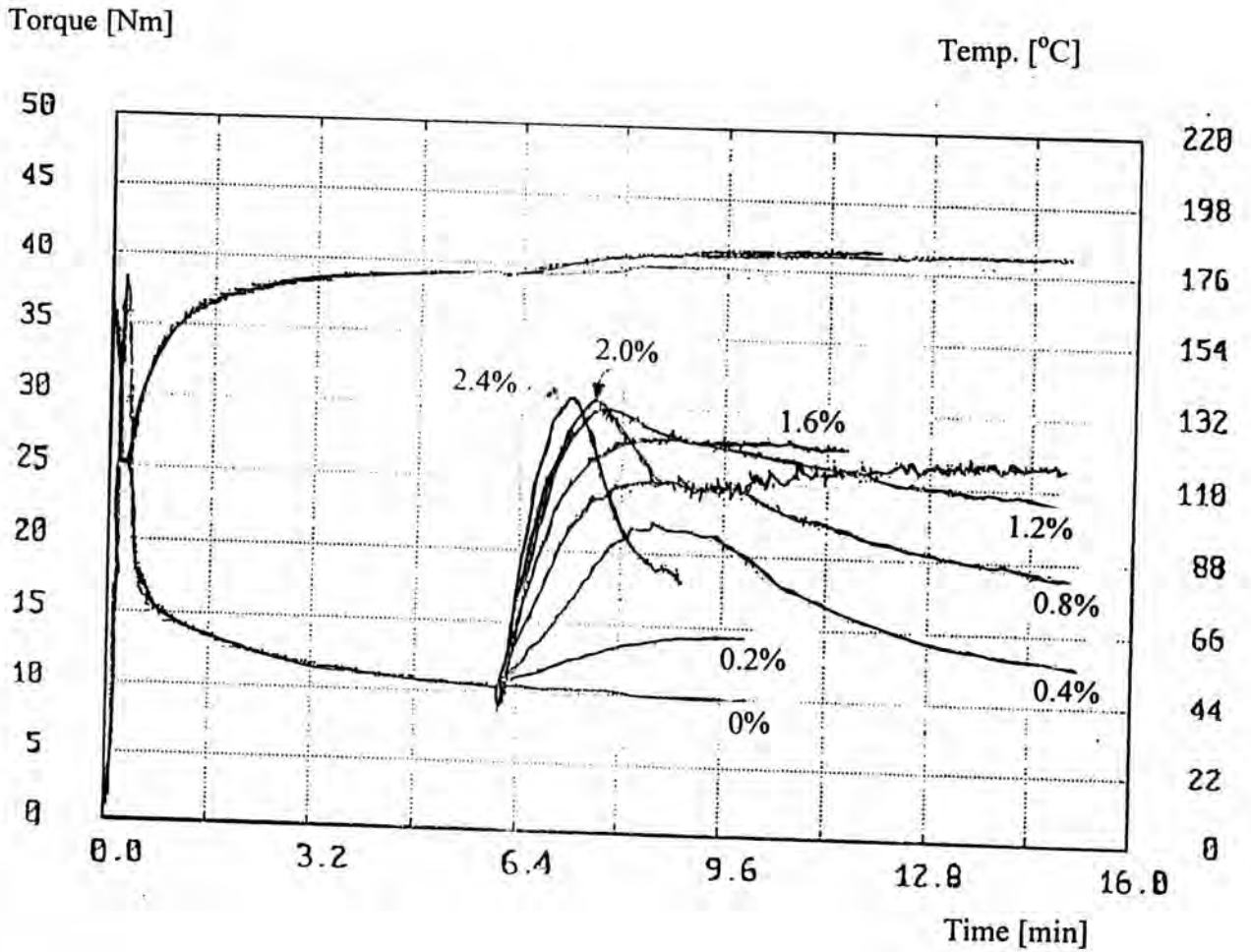
Figure 4.4 Variation of torques during crosslinking of LDPE at various DCP
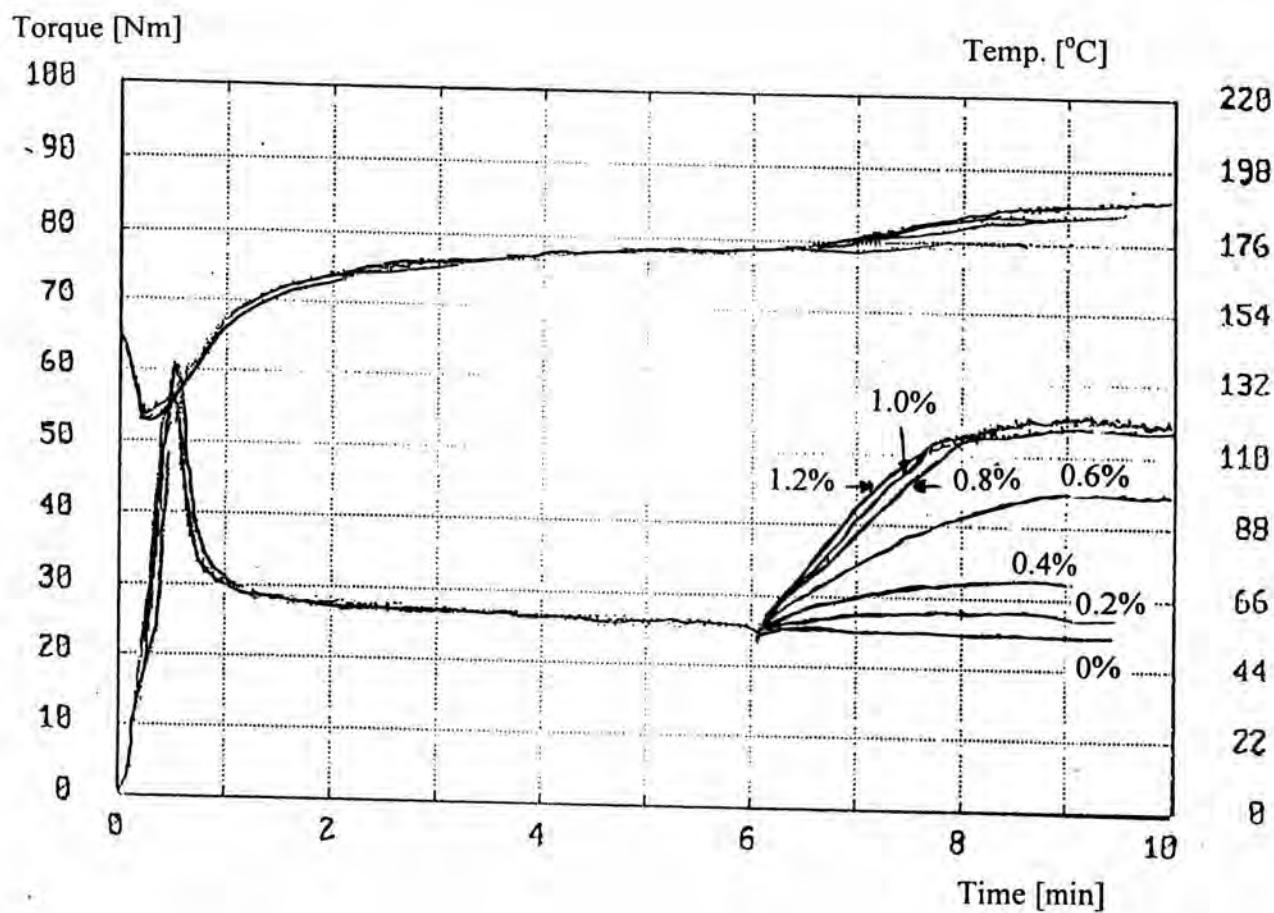concentrations : 446 K , mixer speed of 50 rpm.

Figure 4.5 Variation of torques during crosslinking of LLDPE at various DCP concentrations : 446 K , mixer speed of 50rpm.
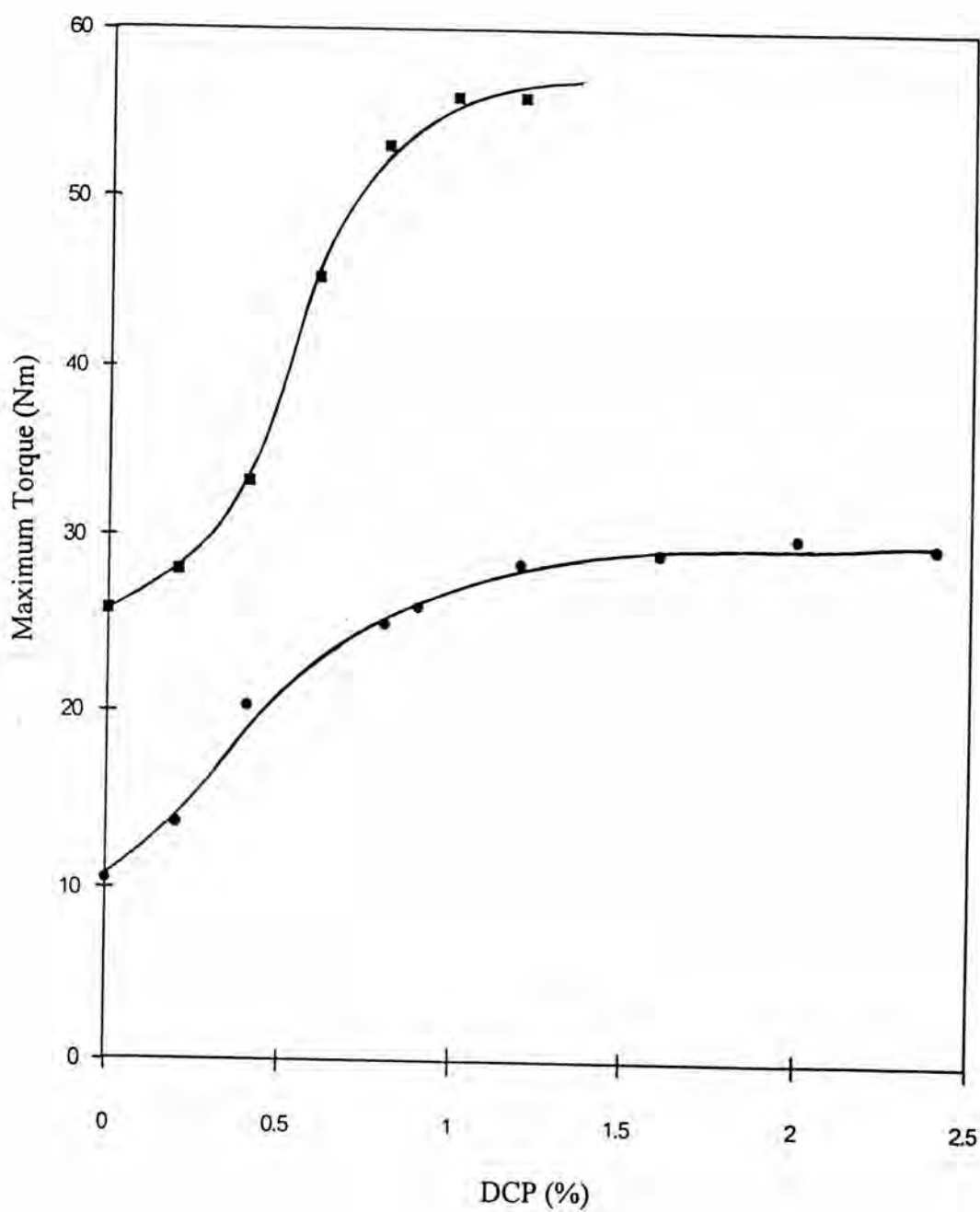
Figure 4.6 Plot of maximum torque during crosslinking reaction of LDPE (•) and
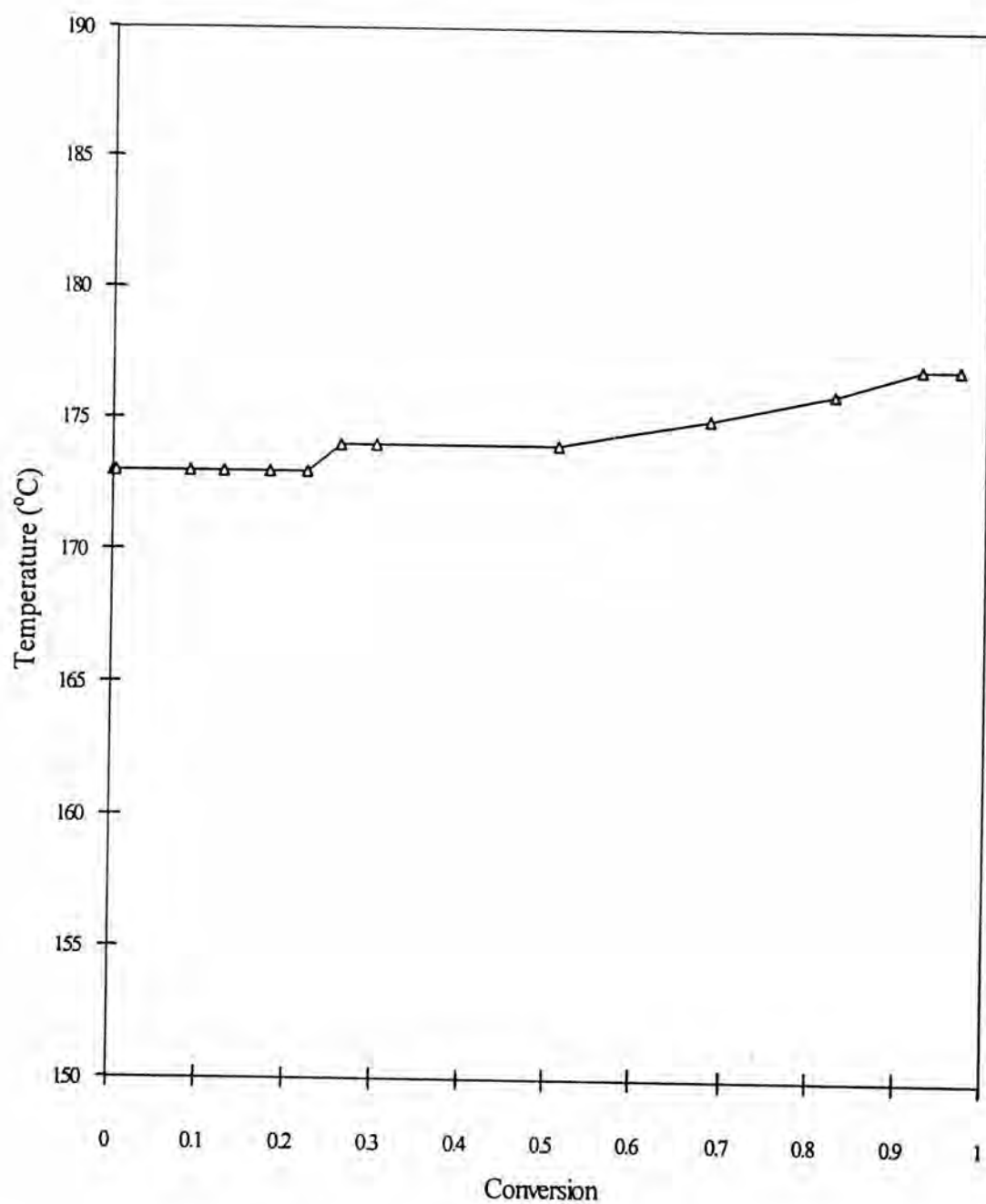LLDPE (■) versus DCP loading at 446 K and mixer speed 50rpm.

Figure 4.7 Variation of polymer temperature at various crosslinking conversion; DCP 2.0%, and mixer speed of 50 rpm.
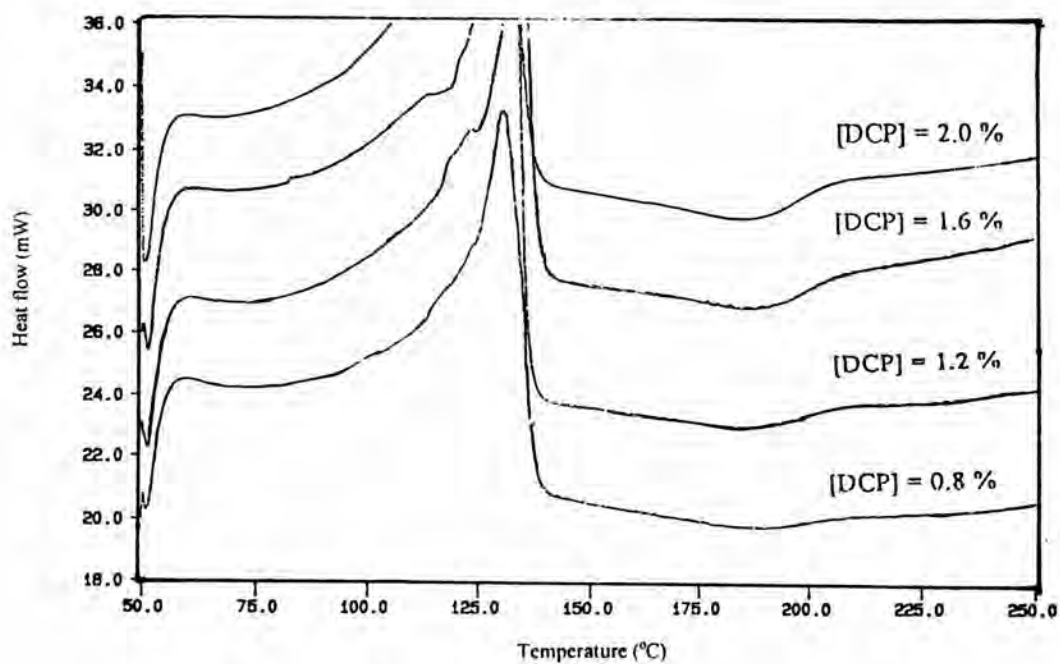
Figure 4.8 DSC thermograms of the crosslinking reaction of LDPE at various DCP concentrations.
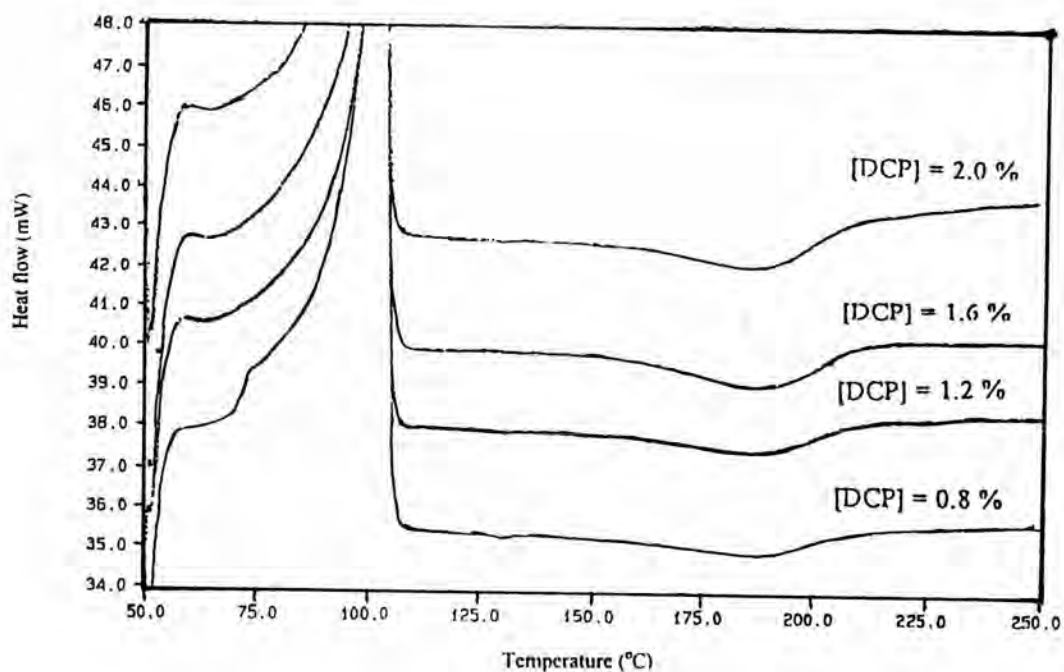

Figure 4.9 DSC thermograms of the crosslinking reaction of LLDPE at various DCP concentrations.

Table 4.1 Total heat of reaction of LDPE and LLDPE at various DCP concentrations.

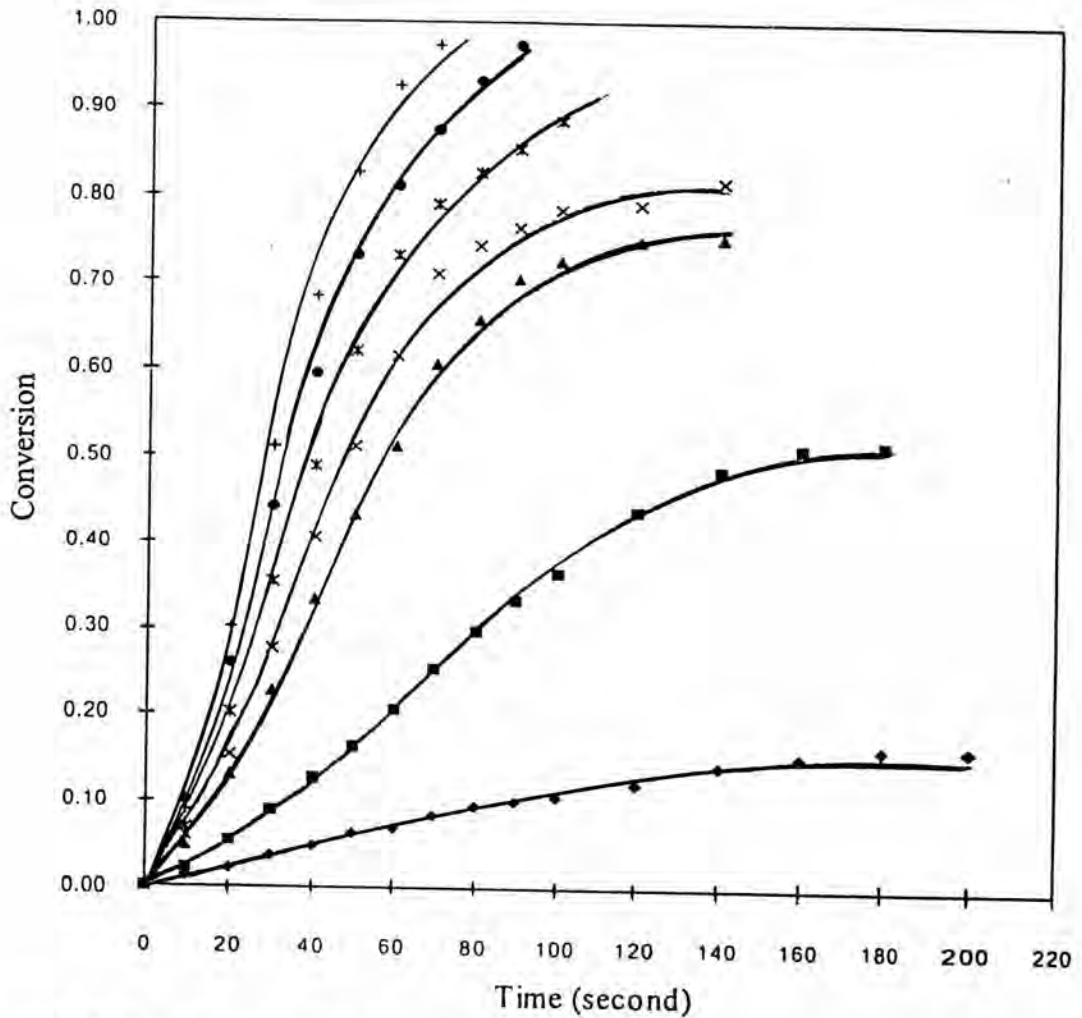| DCP	Total heat of reaction (J/g)	
(%)	LDPE	LLDPE
0.8	6.432	7.014
1.2	7.051	8.731
1.6	9.414	10.311
2.0	12.510	12.357

Figure 4.10 Plot of conversion versus time for LDPE crosslinking reaction at 446 K at various DCP concentrations : ◆, 0.20%; ■, 0.40%; ▲, 0.8%; ×, 0.9%; ✳,1.2%; ●,1.6%; +,2.0%;. (Rheometric technique)
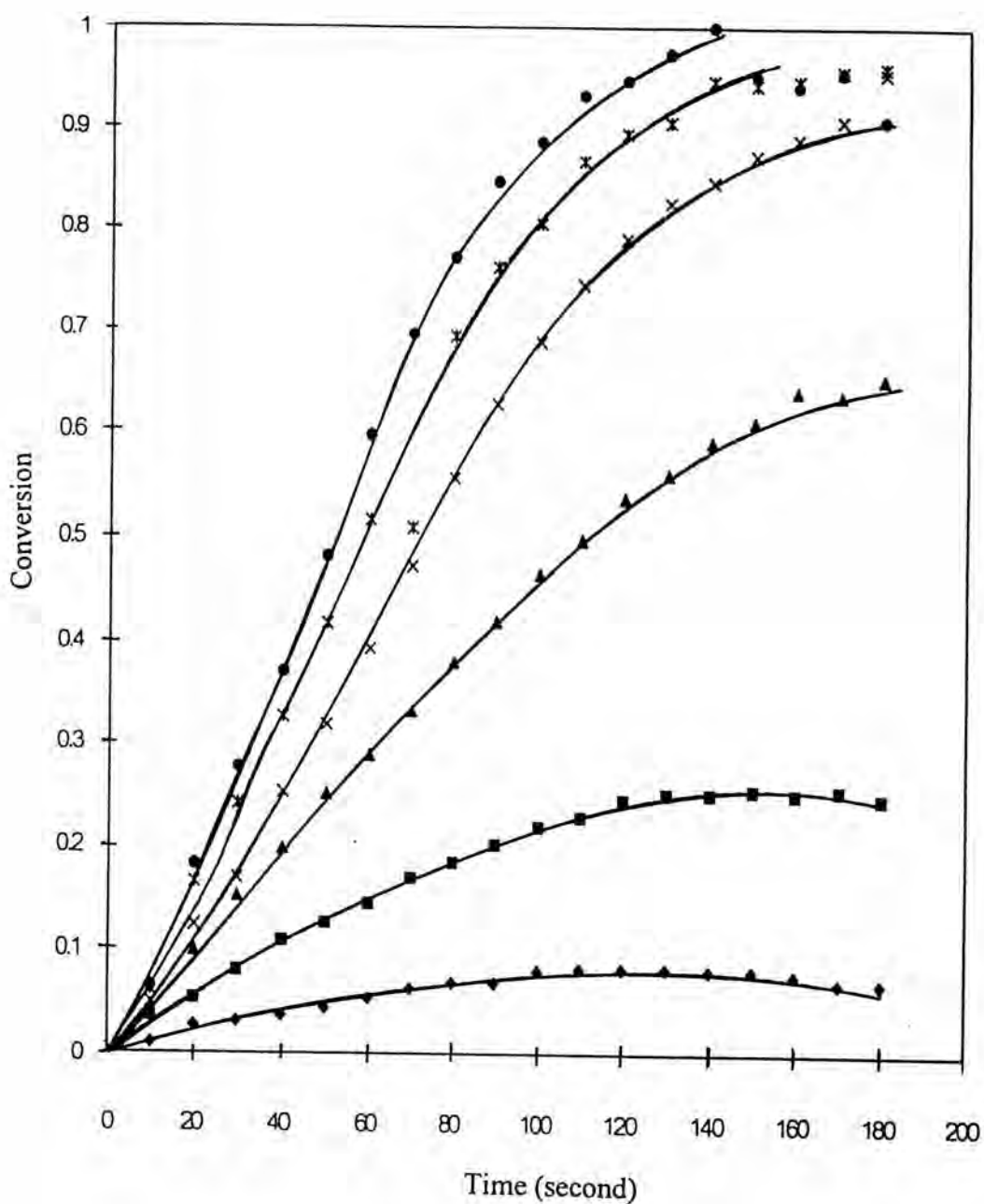
Figure 4.11 Plot of conversion versus time for LLDPE crosslinking reaction at 446 K at various DCP concentrations: ♦, 0.20%; ■, 0.40%; ▲, 0.60%; ×, 0.8%; ∗, 1.0%; ●,1.2%.(Rheometric technique)
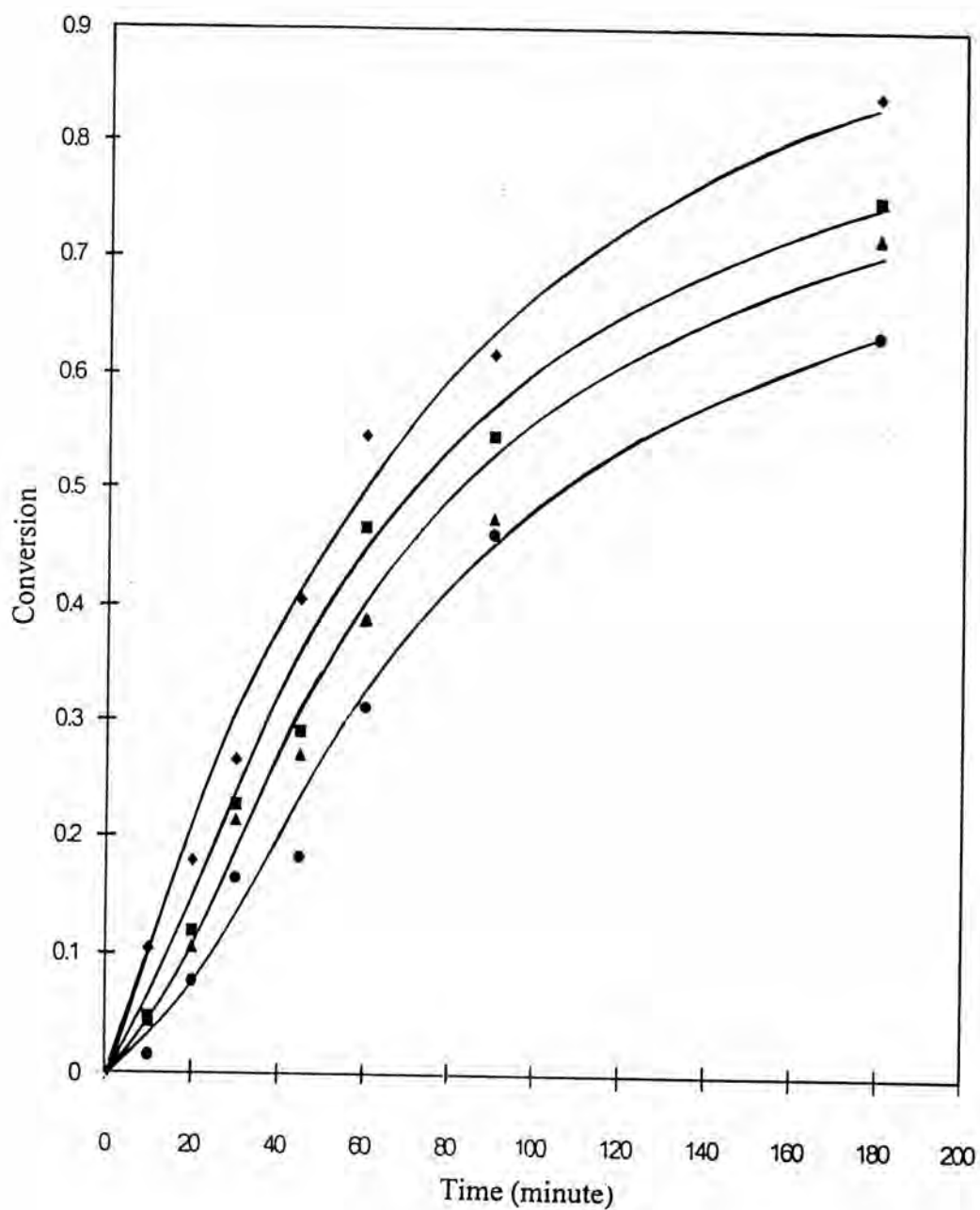
Figure 4.12 Plot of conversion versus time for LDPE crosslinking reaction at 413K at the various of DCP concentrations : ●, 0.8%; ▲, 1.2%; ■, 1.6%; ◆, 2.0%. (DSC technique)
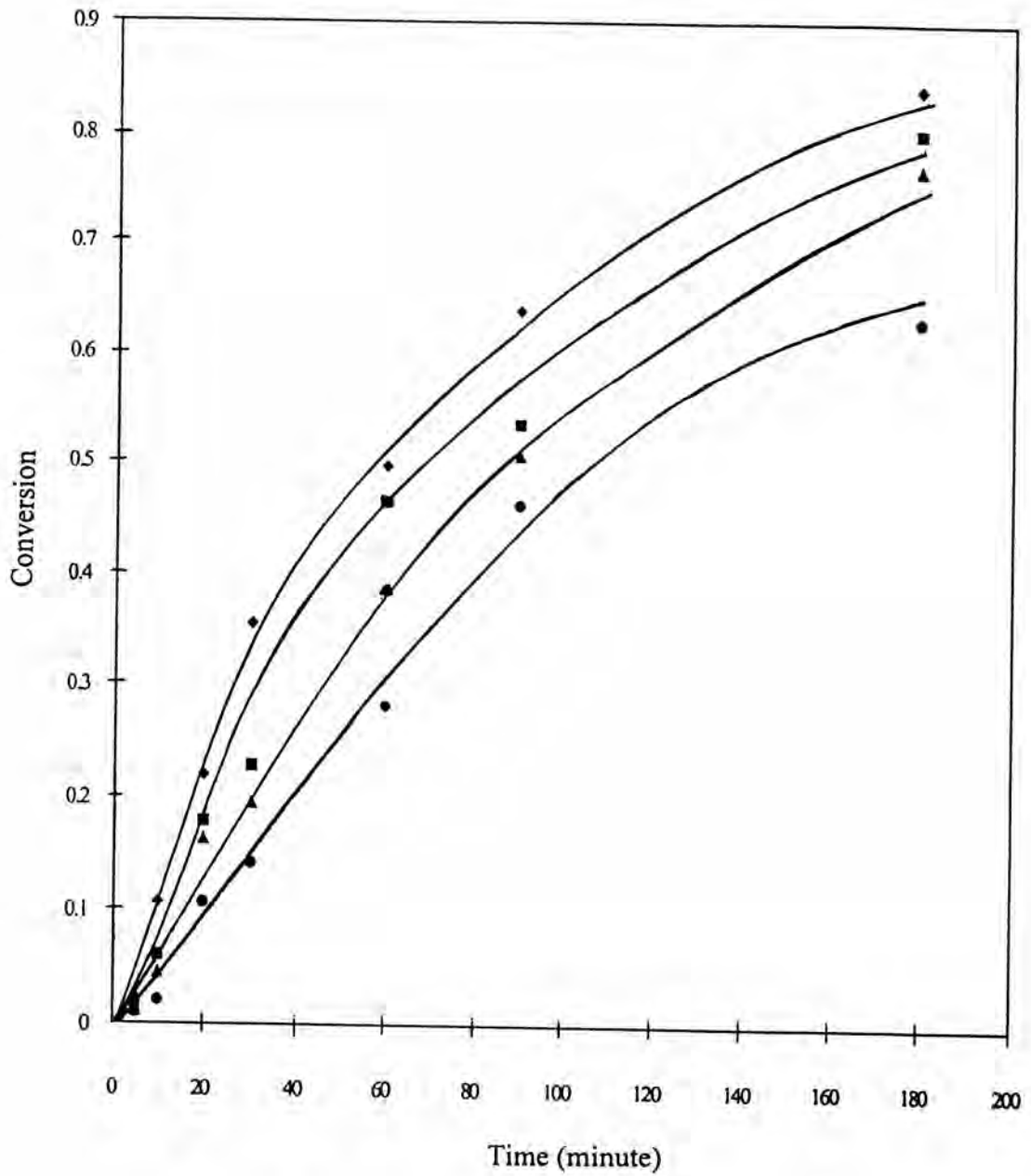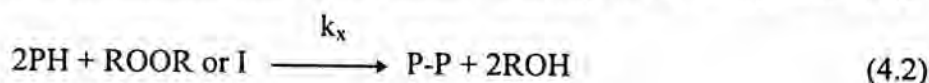
Figure 4.13 Plot of conversion versus time for LLDPE crosslinking reaction at 413K
at various DCP concentrations : ●, 0.8 %; ▲, 1.2%; ■, 1.6%; ◆, 2.0%.
(DSC technique)

a) Determination of reaction order with respect to initiator concentration

The overall crosslinking reaction equation can be expressed in Equation (4.2).

$$2PH + ROOR \text{ or } I \xrightarrow{k_x} P\text{-}P + 2ROH \tag{4.2}$$

where k_x is the rate constant for the overall crosslinking reaction.

The rate of crosslinking reaction R_x is synonymous to the rate of polymer disappearance $(-d[PH]/dt)$, i.e.,

$$R_x = -d[PH]/dt = k_x[PH]^m[I]^n \tag{4.3}$$

where [PH] and [I] are the polymer and the initiator concentrations, respectively and m and n are the exponent order of the polymer and initiator concentration, respectively.

The conversion relates to the rate of crosslinking reaction as shown in Equation (4.4).

$$R_x = -d[PH]/dt = [PH]_0 \, (dx/dt) \tag{4.4}$$

where $[PH]_0$ is the initial concentration of polymer.

Let's k'_x equals to $k_x/[PH]_0$, and k'_x is the rate constant for the overall crosslinking reaction in the absence of inhibitor. Substitution of Equation (4.4) into Equation (4.3) yields

$$dx/dt = k'_x[PH]^m[I]^n \tag{4.5}$$

Take natural logarithm of Equation (4.5), one obtains

$$\ln(dx/dt) = \ln(k'_x[PH]^m) + n \ln[I] \tag{4.6}$$

For the rheometric technique, the plot of ln(dx/dt) against ln([I]) at 446 K is shown in Figure 4.14. The similar plot at 413 K for the DSC technique is shown in Figure 4.15. Since dx/dt is the initial rate of crosslink reaction, the conversion was limited to less than 10 %. These plots were used to evaluate the value of the exponent order of DCP from the slopes, which in this work, it was first order independent upon either the types of polyolefins or the techniques used for the studies.

	Slope	Intercept	R-square
LDPE	1.04	-5.16	0.988
LLDPE	1.06	-5.08	0.966
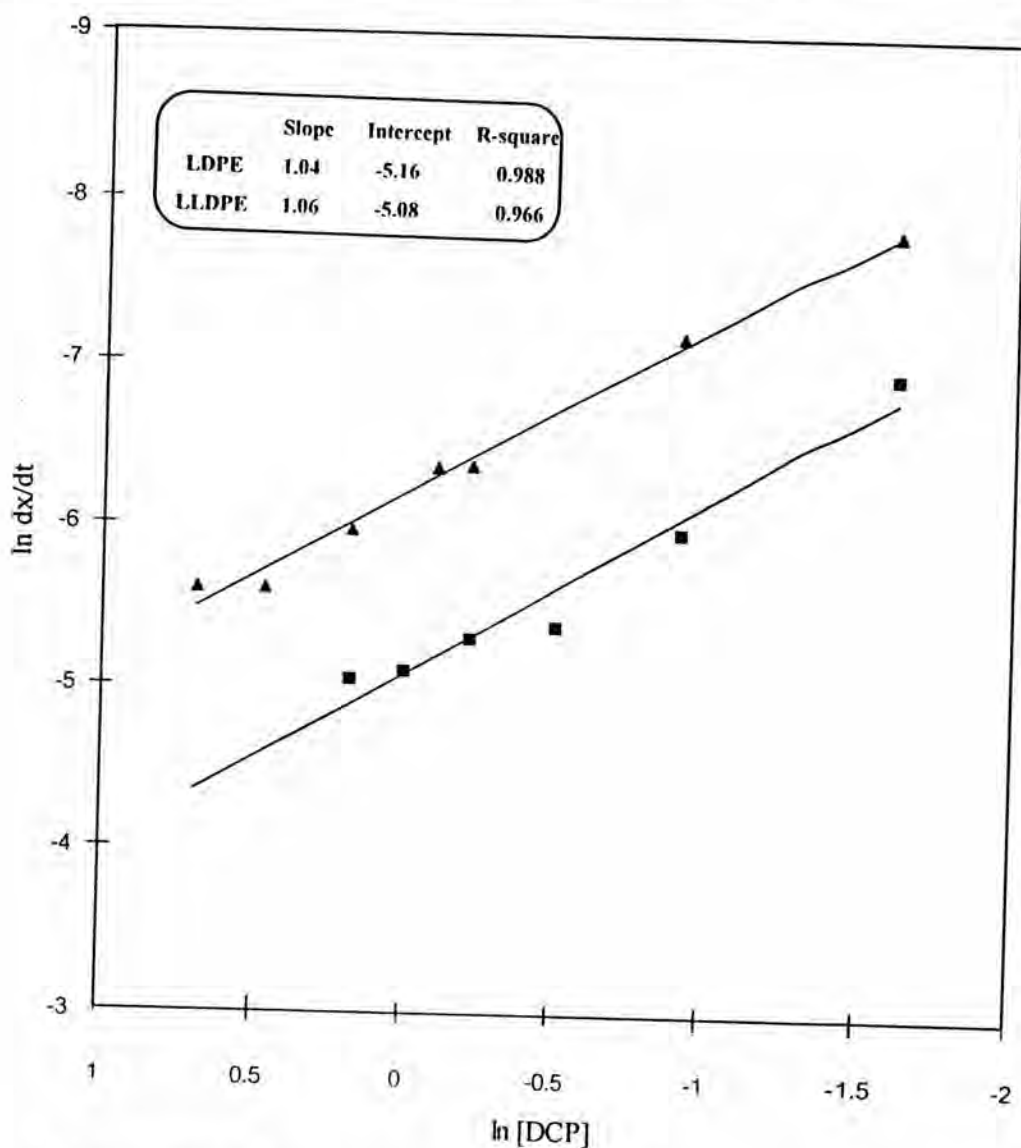
Figure 4.14 Plot of ln(dx/dt) versus ln[DCP] at 446 K.: ▲, LDPE; ■, LLDPE. In order to prevent overlap, ln(dx/dt) for LDPE is subtracted with 1. (Rheometric technique)
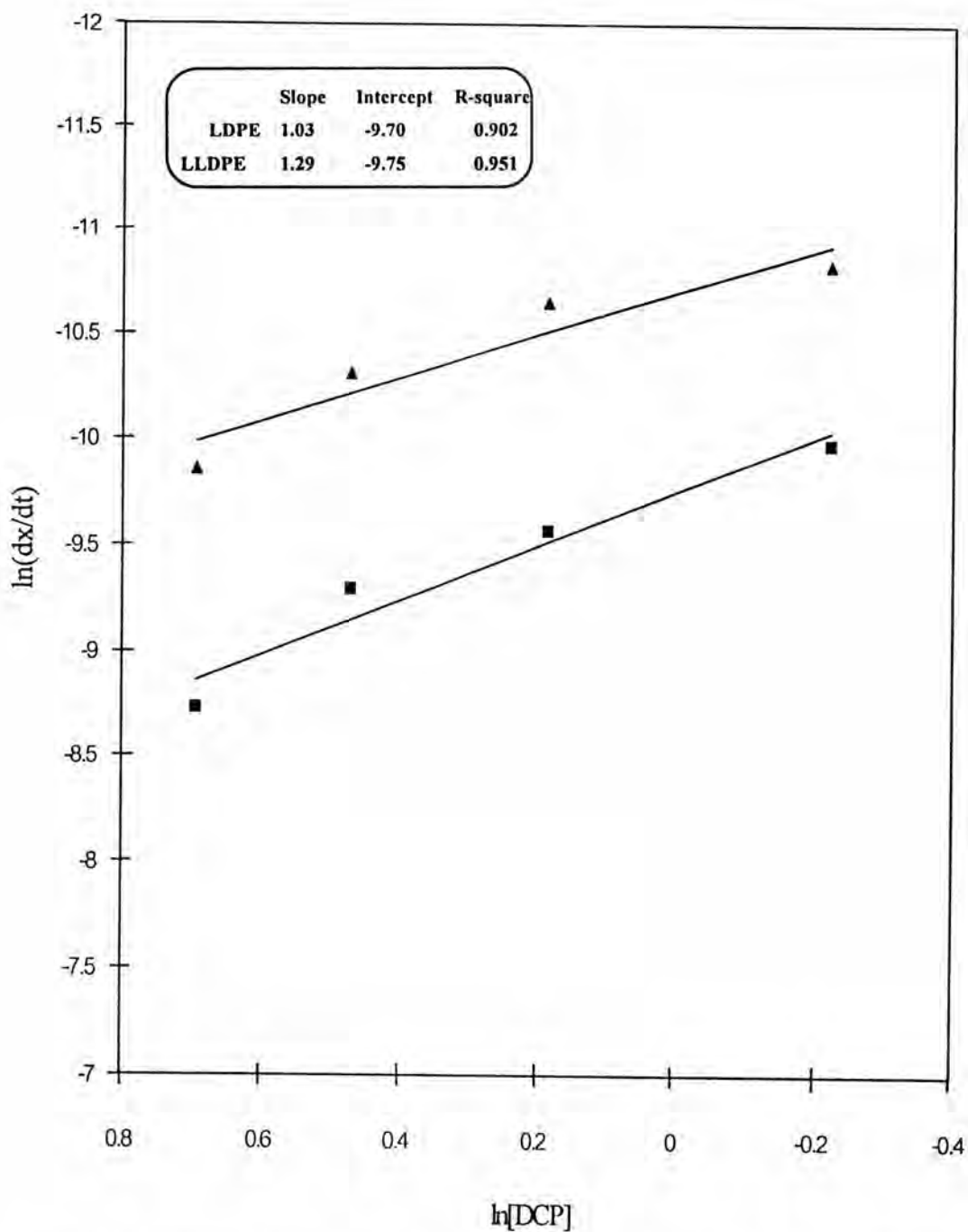
Figure 4.15 Plot of ln(dx/dt) versus ln[DCP] at 413 K : ▲, LDPE; ■, LLDPE. In order

to prevent overlap, ln(dx/dt) for LDPE is substracted with 1.

(DSC technique)

b) Determination of reaction order with respect to polymer concentration

Substitutions of the value of n equal to unity and of $[I] = I_0 e^{-k_d t}$ (Equation (2.21)) into Equation (4.3) gives

$$\frac{-d[PH]}{dt} = k_x [PH]^m I_0 e^{-k_d t} \qquad (4.7)$$

Integration of the above equation with the boundary of $[PH]_{t=t} = [PH]$ and $[PH]_{t=0} = [PH]_0$ yields

$$\frac{-([PH]^{1-m} - [PH]_0^{1-m})}{1-m} = k_x I_0 (1 - e^{-k_d t}) \qquad (4.8)$$

Substitution of $x = ([PH]_0 - [PH])/[PH]_0$ into Equation (4.8), one obtains

$$\frac{-([PH_0]^{1-m} ((1-x)^{1-m} - 1))}{1-m} = k I_0 (1 - e^{-k_d t}) \qquad (4.9)$$

Rearrangement of the above equation yields

$$\frac{-((1-x)^{1-m} - 1)}{1-m} = \frac{k_x I_0 (1 - e^{-k_d t})}{([PH_0]^{1-m}} \qquad (4.10)$$

Since the exponent order m of the term [PH] was not definitely known, it was assumed to be 0 to 3 step 0.5. Substitutions of those values into the left-hand-side of Equation (4.9) yield x, $1-(1-x)^{0.5}$, $-\ln(1-x)$, $(1/(1-x)^{0.5}-1)$, $x/(1-x)$, $(1/(1-x)^{1.5} -1)$ and $(1/(1-x)^2-1)$. The plots of these terms versus $(1-e^{-k_d t})$ are shown in Figures 4.16 and 4.17 for the Rheometric technique. The value of k_d was obtained from Akzo Chemicals Ltd.[16] to be 7.20×10^{-3} sec^{-1}. When the value of m was assumed equal to zero, a linear correlation was obtained. This evidence indicated clearly that the reactions were independent upon the polymer concentration. In conclusion the peroxide crosslinking reactions of LDPE and LLDPE in the absence of an inhibitor followed the first order kinetics which was found by many investigators [19, 20, 25].

In the other words, the crosslinking reaction depends only upon the rate of initiator dissociation reaction, which is the rate determining step. Equation (4.3) simplifies to

$$R_x = k_x[I] \qquad (4.11)$$

which has been derived theoretically as shown in Equation (2.31).

Equation (4.6) also simplifies as shown in Equation (4.12).

$$\ln(dx/dt) = \ln k'_x + \ln [I] \qquad (4.12)$$

so that the values of k'_x, given in Table 4.2, can be evaluated from the intercepts of the linear plots shown in Figures 4.14 (RHE) and 4.15 (DSC).

Table 4.2 The values of rate constants for crosslinking reaction of LDPE and LLDPE.

Technique	Temperature (K)	k'_x (sec)$^{-1}$	
		LDPE	LLDPE
Rheometric	446	5.74×10^{-3}	6.22×10^{-3}
DSC	413	6.15×10^{-5}	5.83×10^{-5}
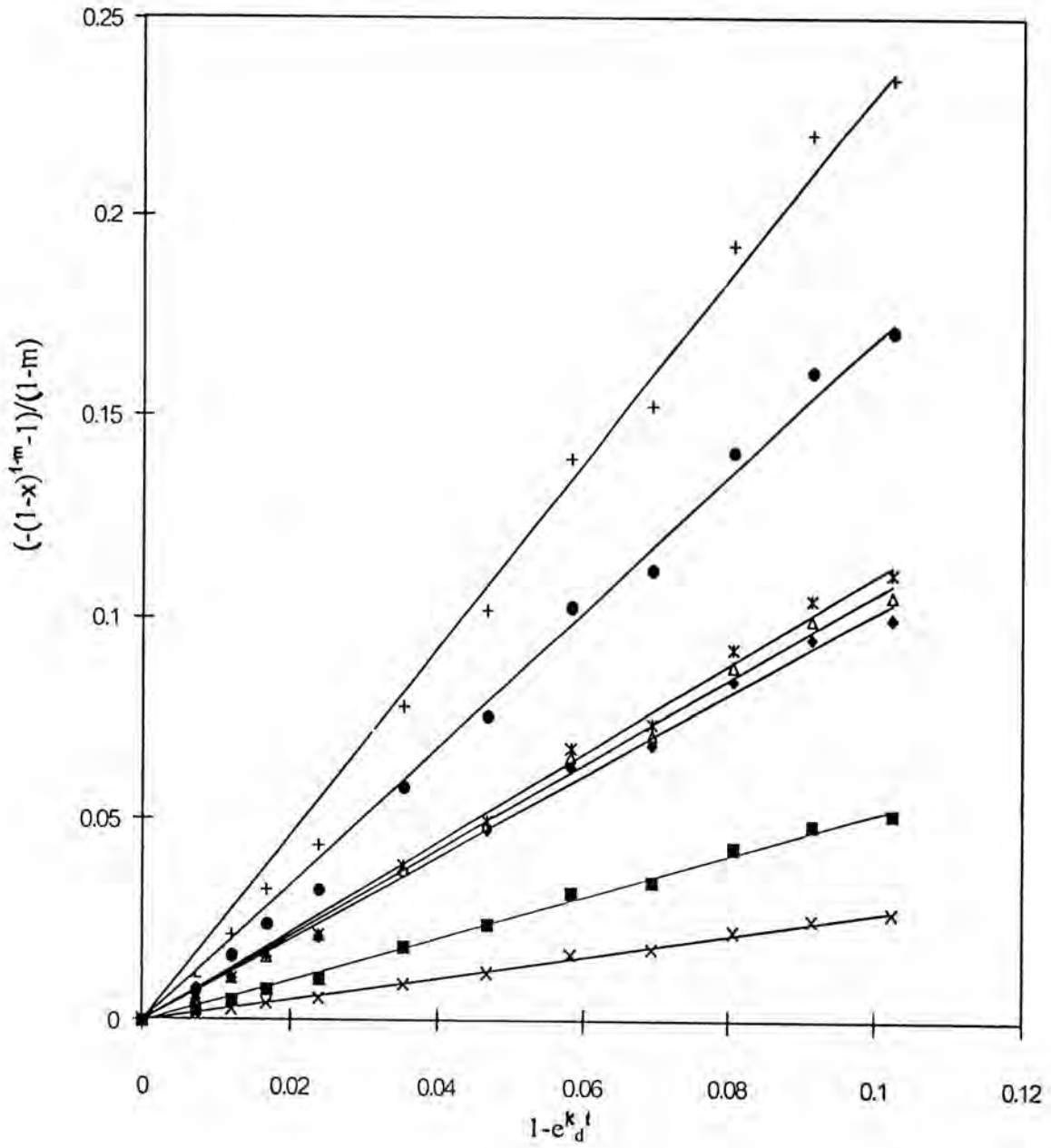
Figure 4.16 Plot of $(-(1-x)^{1-m}-1)/(1-m)$ versus $1-e^{-k_d t}$ for LDPE crosslinking at 446 K, 0.2% DCP: m = ♦, 0; ■, 0.5; ▲, 1; ×, 1.5; ✱, 2; ●, 2.5; +, 3. (Rheometric technique)
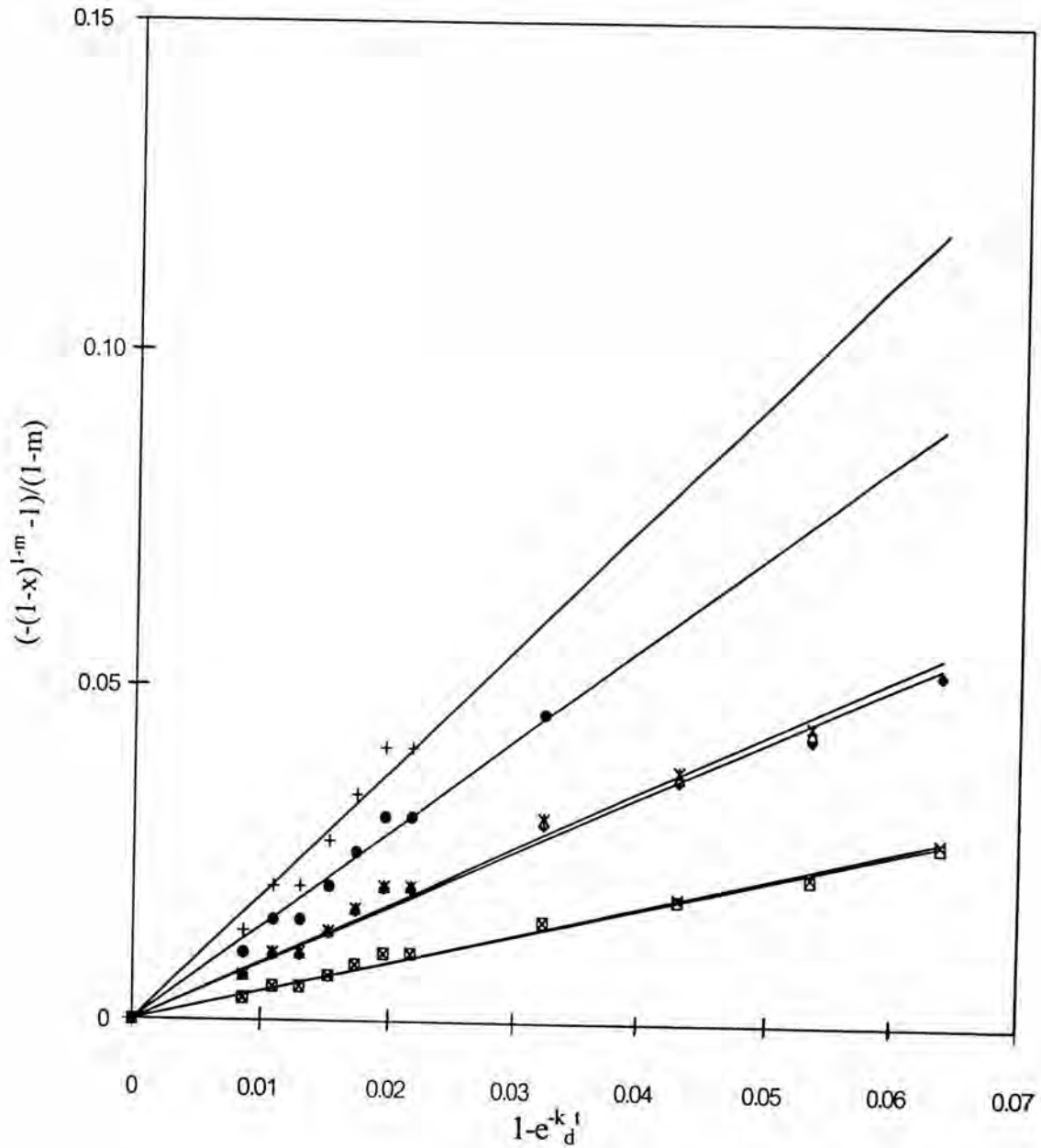
Figure 4.17 Plot of $(-(1-x)^{1-m}-1)/(1-m)$ versus $1-e^{-k_d t}$ for LLDPE crosslinking at 446 K,

0.2% DCP: m = ◆, 0; ■, 0.5; ▲, 1; ×, 1.5; ✳, 2; ●, 2.5; +, 3.

(Rheometric technique)

4.3.2 Kinetics of Crosslinking Reaction in the Absence of an Inhibitor at Various Temperatures

Figures 4.18-4.19 and 4.20-4.21 show the conversion-time plots at various reaction temperatures for Rheometric and DSC technique, respectively. The rate constants at various temperatures are given in Table 4.3. They were determined from the relationship shown in Equation (4.13).

$$(dx/dt) = k'_x[I] \qquad (4.13)$$

Table 4.3 The values of rate constants for crosslinking reaction at various temperatures.

Material	RHE		DSC	
	Temperature (K)	$k'_x \times 10^3$ $(sec)^{-1}$	Temperature (K)	$k'_x \times 10^5$ $(sec)^{-1}$
LDPE	446	5.50	393	0.59
	455	10.0	403	2.22
	464	24.0	413	7.15
	473	33.4	423	34.3
LLDPE	446	5.00	393	0.70
	455	14.5	403	2.93
	464	23.0	413	8.10
	473	31.0	423	35.5

The Arrhenius plots shown in Figures 4.22 and 4.23, i.e., ln(dx/dt) versus 1/T, allow to determine the overall activation energy E_a and pre-exponential factor A, which are presented in Table 4.4.

Table 4.4 The values of E_a and A of crosslinking reaction of LDPE and LLDPE using Rheometric and DSC techniques.

Technique	LDPE		LLDPE	
	E_a (kJ/mol)	A (sec^{-1})	E_a (kJ/mol)	A (sec^{-1})
RHE	118	3.23×10^{11}	112	0.82×10^{11}
DSC	184	3.56×10^{19}	176	3.64×10^{18}

The values evaluated by the DSC technique were higher than those by the other method might be due to

1) The convection parameter. In the BPC mixing chamber, the heat convection through materials could accelerate the crosslinking reaction, leading to the decrease of the activation energy.

2) The method used to determine the crosslink conversion. For BPC technique, the conversions were determined from the changes of torques during the crosslinking reaction depending on the melt viscosity of the materials or their molecular weight presented in the mixing chamber. The crosslinked polymers were achieved by the combination reaction of two polymer radicals, which in fact contributed to the changes of torques. Disproportionation or cyclization of those radicals did not affect the changes of torques since the final polymers obtained had similar molecular weight to the polymer radicals. Whilst, in the DSC, the conversions were determined from the changes of heat of reactions which composed of the heat from DCP dissociation reaction and of the carbon-carbon bond formation which involved the combination, disproportionation and cyclization reactions. Therefore, the values of collision frequency or pre-exponential factor evaluated from the DSC technique should be higher than those determined from the other.

Assumptions were made in that a) the shear force during the experiments contributed equally on the rates of combination, disproportionation, and cyclization, b) the polymer radicals that was initiated by shearing was lower than those initiated from the hydrogen abstraction by peroxy radicals and c) the degradation of crosslinked polymer by shearing would not occur during the crosslinking reaction unless the peroxide compound was depleted. The relative difference of E_a obtained from

DSC and BPC techniques was found to be 35.9% for LDPE and 36.4% for LLDPE. This implied that the combination of polymer radicals occurred about 65%, while around 35% was due to the other terminations. Vandrumpt and coworkers [19] reported that approximately 50-60% of the hydrogen abstracted n-alkane were found subject to the combination, while, Hulse and coworkers [31] found that the intermolecular coupling was about 40% for an alkane and 25-30% for polymer.

The higher values obtained from this study might be due to the polymer radicals occurred by mechanical shearing and then they could combine together. If polymer radicals were terminated by cyclization and disproportionation, it would not affect to the torque. In conclusion, the polymer radicals were not only occurred from the peroxide-initiated reaction but also from the mechanical shear.
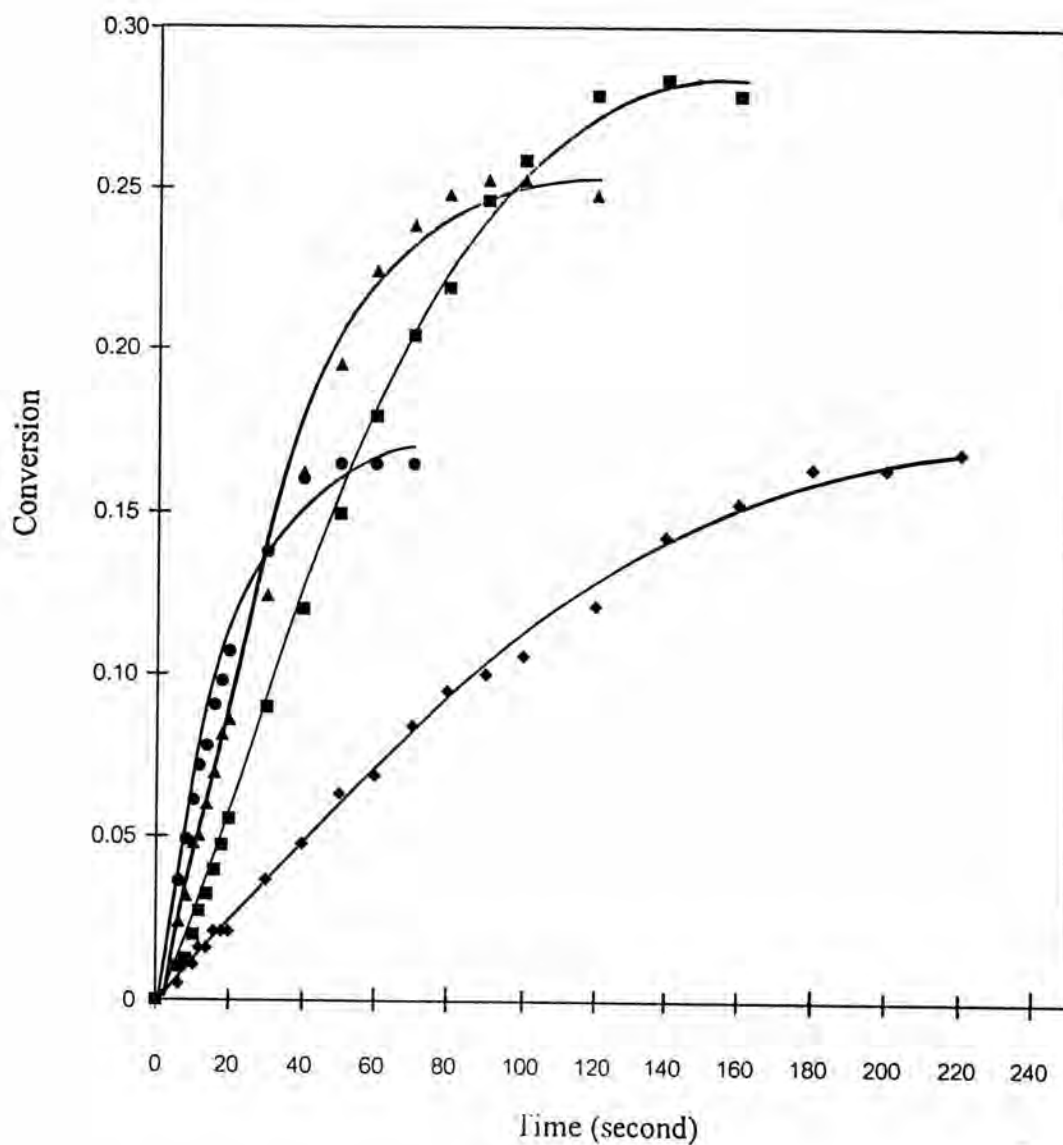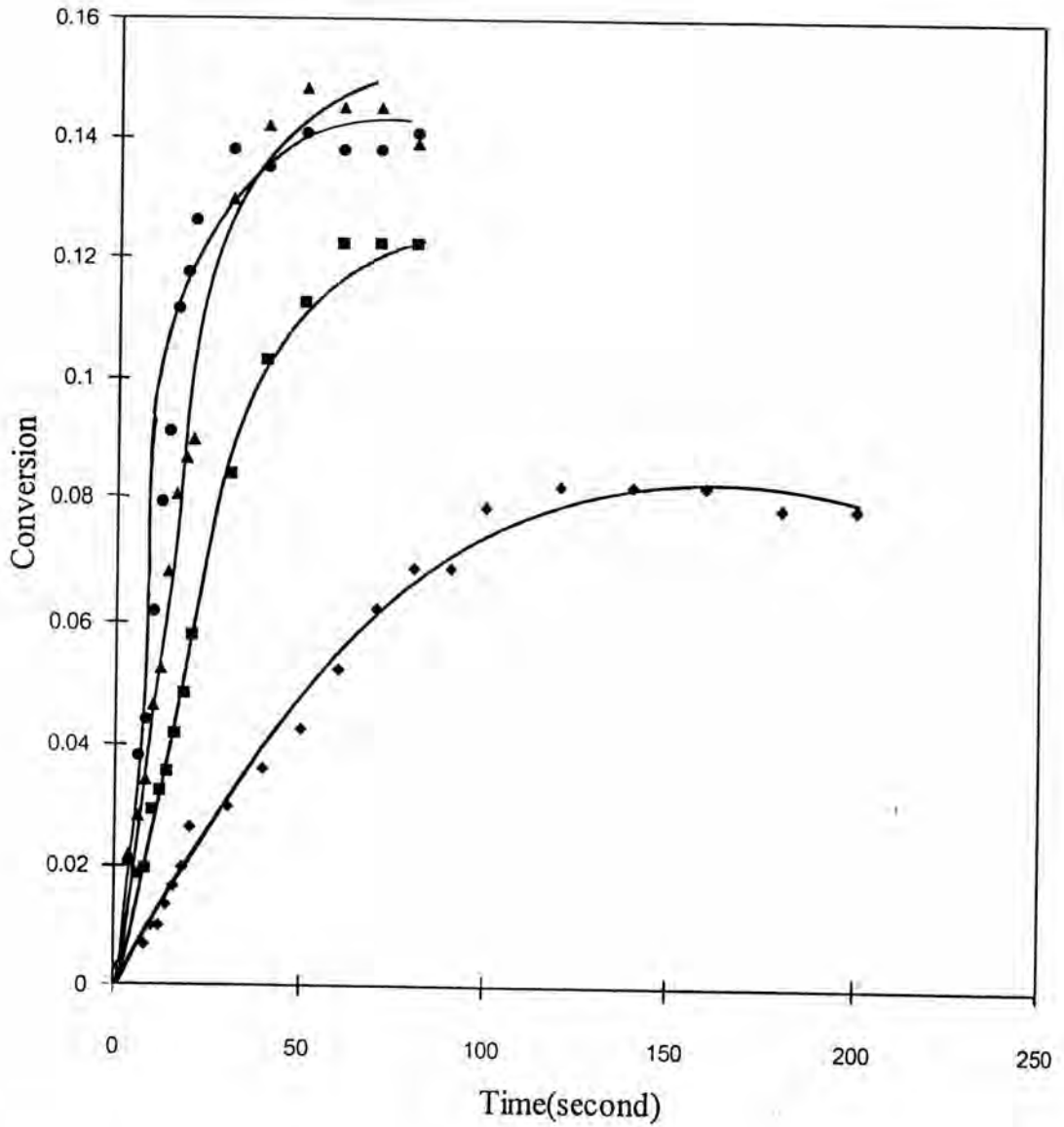
Figure 4.18 Plot of conversion versus time for LDPE crosslinking at various temperatures, 0.2% DCP: ♦, 446 K; ■, 455 K; ▲, 464 K; ●, 473 K. (Rheometric technique)

Figure 4.19 Plot of conversion versus time for LLDPE crosslinking at various temperatures, 0.2% DCP: ◆, 446 K: ■, 455 K; ▲, 464 K; ●, 473 K. (Rheometric technique)
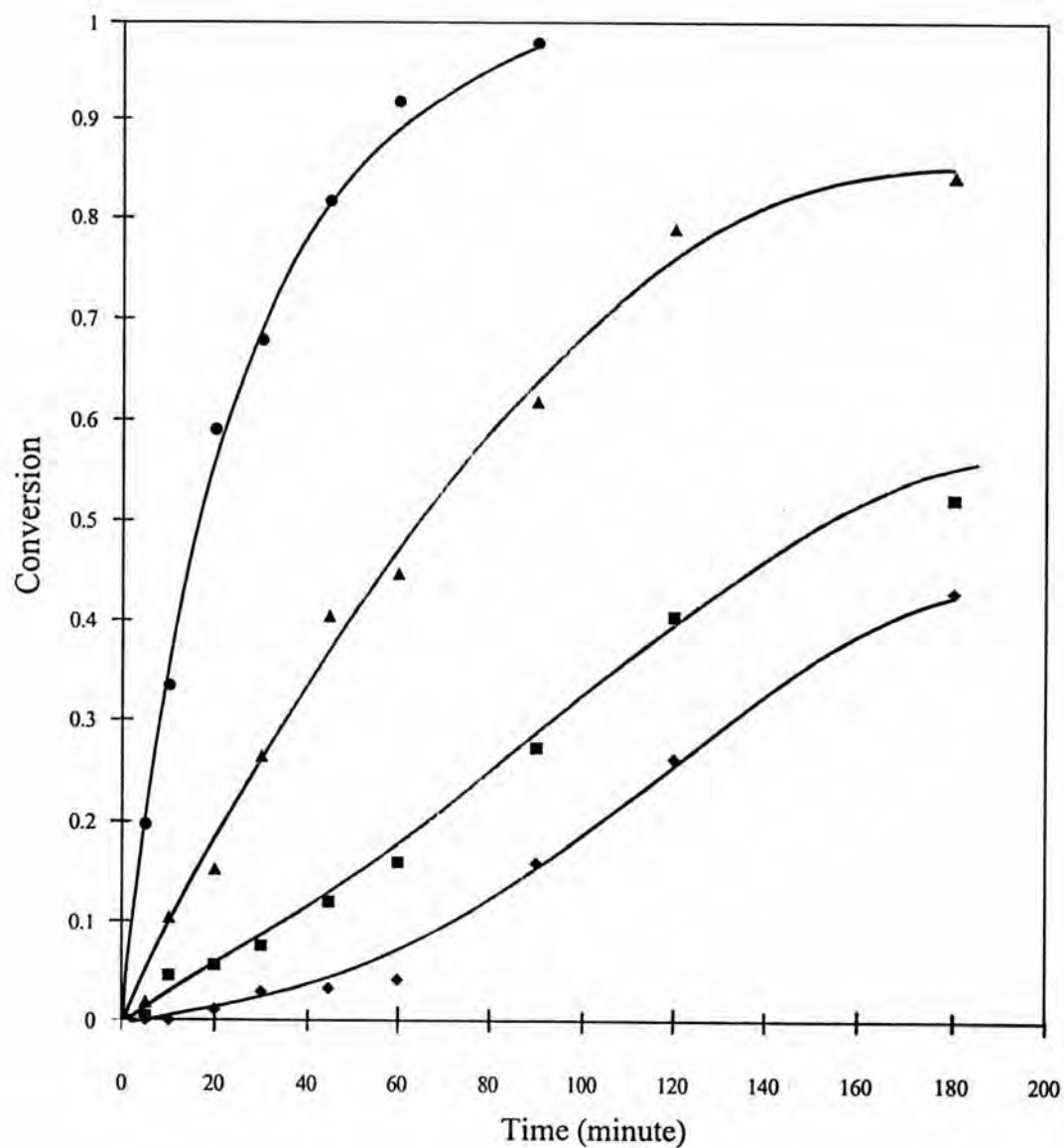
Figure 4.20 Plot of conversion versus time for LDPE crosslinking at various
temperatures, DCP 2.0%: ♦, 393K; ■, 403K; ▲, 413K; ●, 423K.
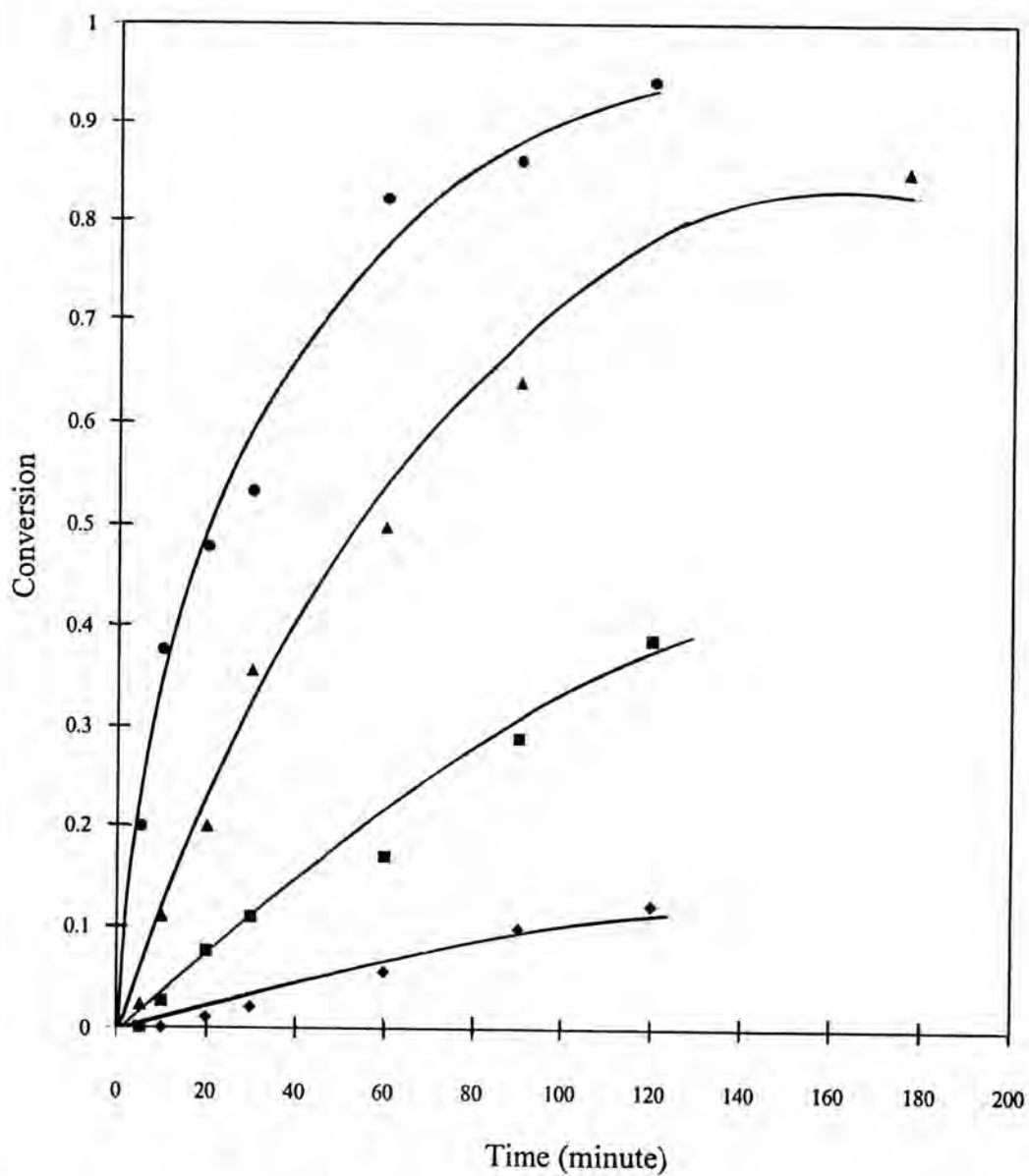(DSC technique)

Figure 4.21 Plot of conversion versus time for LLDPE crosslinking at various

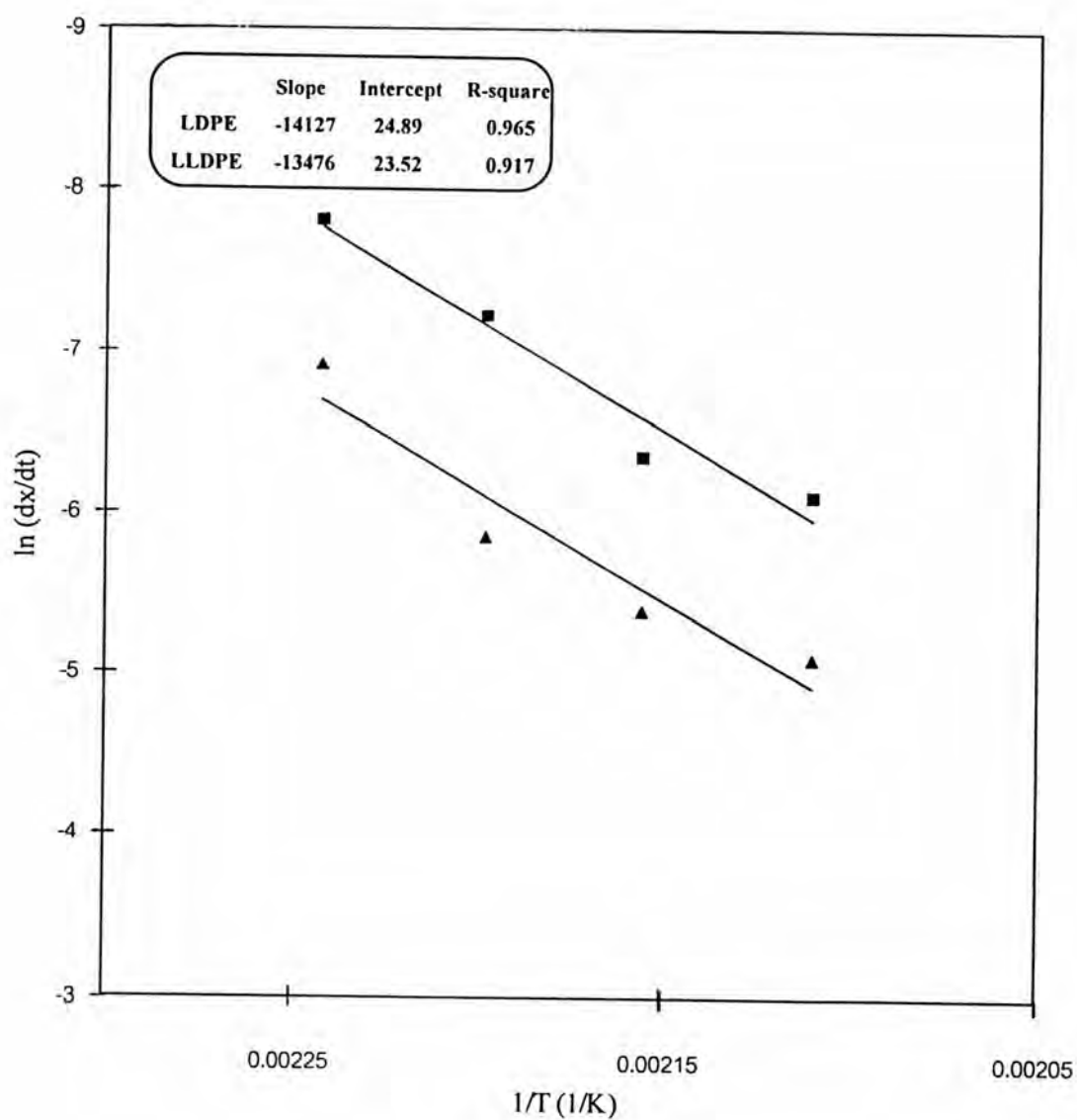temperatures, DCP 2.0%: ♦, 393K; ■, 403K; ▲, 413K; ●, 423K.

(DSC technique)

	Slope	Intercept	R-square
LDPE	-14127	24.89	0.965
LLDPE	-13476	23.52	0.917

Figure 4.22 Arrhenius plot of ln (dx/dt) versus 1/T for crosslinking reaction, 0.2% DCP:■, LDPE; ▲, LLDPE. In order to pervent overlap, ln(dx/dt) for LDPE is substracted with 1. (Rheometric technique)
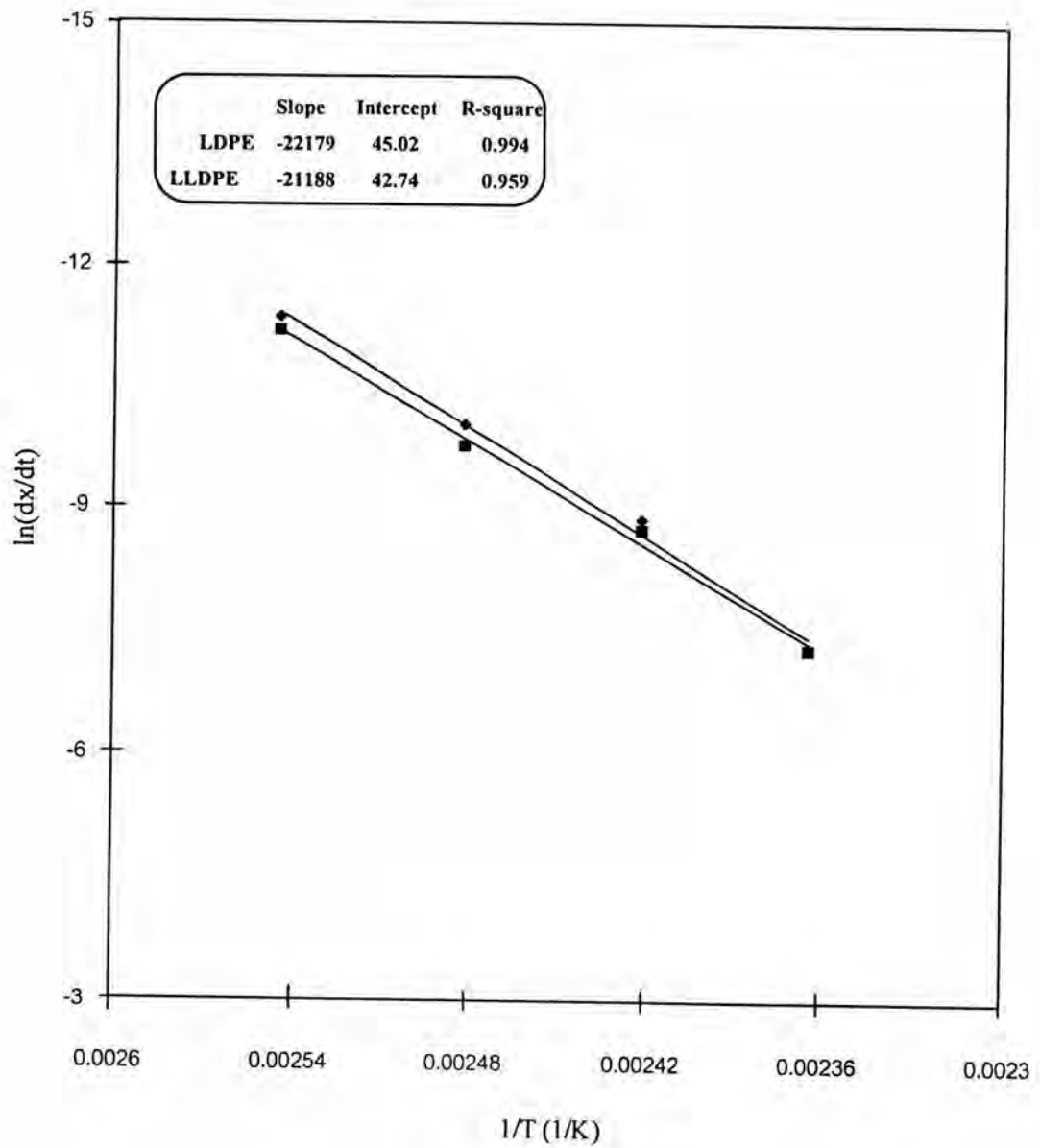
	Slope	Intercept	R-square
LDPE	-22179	45.02	0.994
LLDPE	-21188	42.74	0.959

Figure 4.23 Arrhenius plot of ln (dx/dt) versus 1/T for crosslinking reaction, 0.2% DCP: ◆, LDPE; ■, LLDPE.(DSC technique)

4.3.3 Kinetics of Crosslinking Reaction in the Presence of an Inhibitor

Tetrakis[methylene3-(3'-5'-di-t-butyl-4'-hydroxyphenyl)]propanoate (trade name Irganox 1010) was employed as the inhibitor. The conversions and the rates of the crosslinking reactions of LDPE and LLDPE decreased with the increases of Irganox 1010 concentrations (Figures 4.24-4.25 (RHE) and 4.26-4.27 (DSC)) since it deactivated the active radicals $RO^{\bullet}$ or $P^{\bullet}$ presented in the reaction.

In the presence of an inhibitor Z, Equation (4.5) can be rewritten as

$$dx/dt = k'_{xz}[PH]^m[I]^n[Z]^y \qquad (4.14)$$

where k'_{xz} is equal to $k_{xz}/[PH]_0$, and k'_{xz} is the rate constant for the overall crosslinking reaction in the presence of inhibitor.

Taking the logarithm of the above equation, one obtains

$$\ln(dx/dt) = \ln(k'_{xz}[PH]^m[I]^n) + y\ln[Z] \qquad (4.15)$$

The slope of the ln-ln plots of dx/dt versus ln[Irganox 1010] (Figures 4.28 and 4.29) is the inhibitor order y, which in this study was found to be -0.21 and -0.27 for LDPE and LLDPE for rheometric technique) and -0.23 and -0.31 for LDPE and LLDPE for DSC technique. The minus sign implied that the rate of crosslinking reaction in the presence of inhibitor was inversely proportional to $[Z]^y$. Therefore, Equation (4.14) rearranges to

$$dx/dt = k'_{xz}[PH]^m[I]^n / [Z]^y \qquad (4.16)$$

It has been proved as forementioned that the exponent orders n and m respectively equal to unity and zero, so that Equation (4.16) can be reexpressed for

LDPE and LLDPE as shown in Equations (4.17), (4.18), (4.19) and (4.20), respectively.

For Rheometric technique

LDPE, $\quad dx/dt = k'_{xz}[I] / [Z]^{0.21}$ (4.17)

LLDPE, $\quad dx/dt = k'_{xz}[I] / [Z]^{0.27}$ (4.18)

For DSC technique

LDPE, $\quad dx/dt = k'_{xz}[I] / [Z]^{0.23}$ (4.19)

LLDPE, $\quad dx/dt = k'_{xz}[I] / [Z]^{0.31}$ (4.20)

According to the chemical structure of Irganox 1010 and the inhibition mechanism (see reaction scheme 1), one mole of inhibitor can inhibit four moles of radicals. Consequently, the disappearance rate of one mole of radical is proportional to Irganox 1010 concentration raised to 0.25 power.
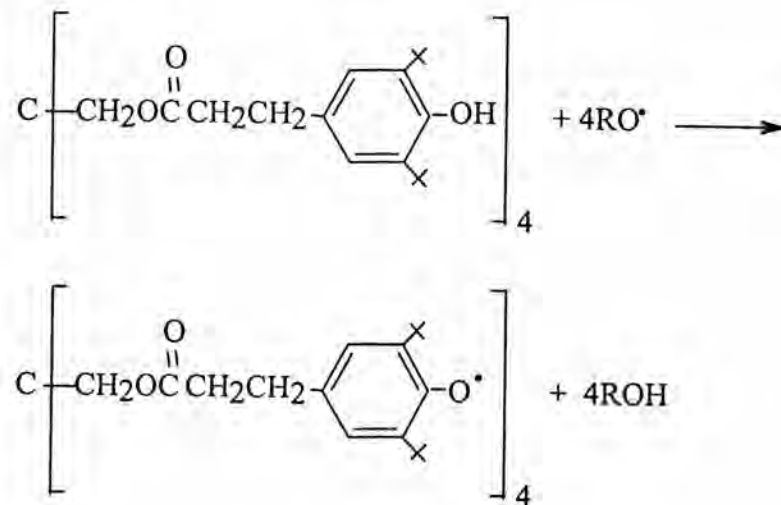
Scheme I

It should be noted that the linearity of the plot of ln(dx/dt) versus ln[Iraganox] obtained from DSC technique was poor . This was attributed to the poor dispersion of Irganox 1010 in polymeric materials. Since the compounding temperature was at 120-125°C so that the time used for dispersion in this study about 2-3 minutes might not

be enough. In addition, since Irganox 1010 has the melting point of 110-125°C, it might not be totally melted during the compounding process.

Since the crosslinking rate was independent upon the polymer concentration, k'_{xz} values at 446 K (Table 4.5) were calculated from the intercept of Equation (4.15).

Table 4.5 Values of rate constant, k'_{xz} at 446 K (Rheometric technique) and 413 K (DSC technique).

Technique	k'_{xz} (sec)$^{-1}$	
	LDPE	LLDPE
RHE	2.11×10^{-3}	2.33×10^{-3}
DSC	4.22×10^{-5}	3.74×10^{-5}

The ratios of k'_x/k'_{xz} were 2.7 (RHE) for LDPE and 2.6 (RHE) for LLDPE indicating that the rate of crosslinking reaction in the presence of Irganox 1010 is around three time slower than that in the absence of inhibitor. The results also suggest that to achieve one intermolecular crosslinking of two polymeric chain requires stoichiometrically three moles of DCP if Irganox 1010 present in the reaction. While in the absence of the inhibitor only one mole of DCP is required. However, these ratio calculated from DSC technique were 1.5 and 1.6 for LDPE and LLDPE, respectively. The different features from those determined by the rheometric technique was due to the poor dispersion of Irganox 1010 in polymeric material as described eariler.
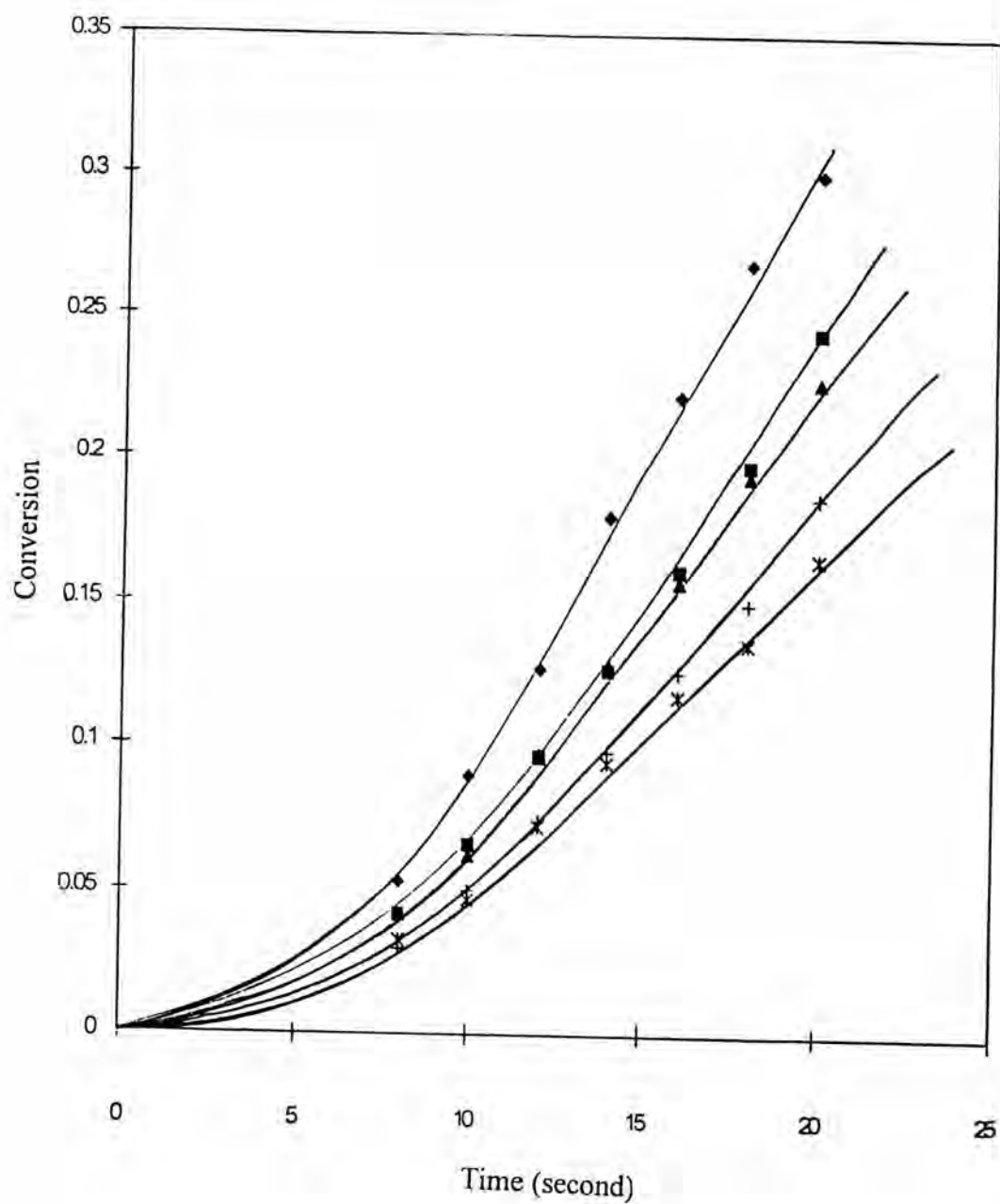
Figure 4.24 Plot of conversion versus time for LDPE crosslinking at various inhibitor concentrations at 446 K, 2.0% DCP; Irganox ♦, 0%; ■,0.10; ▲, 0.20%; +, 0.4%; ✳, 0.6%.(Rheometric technique)
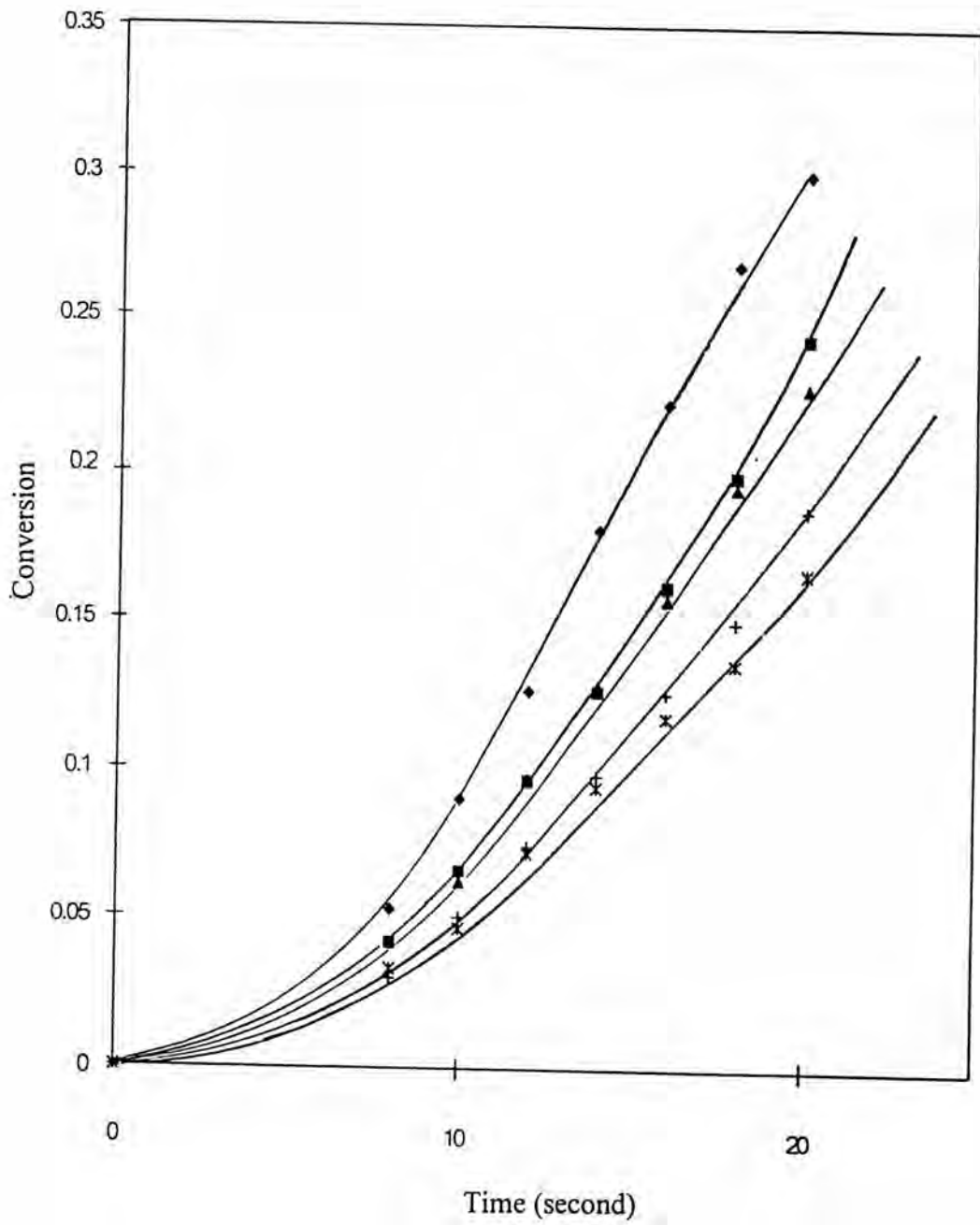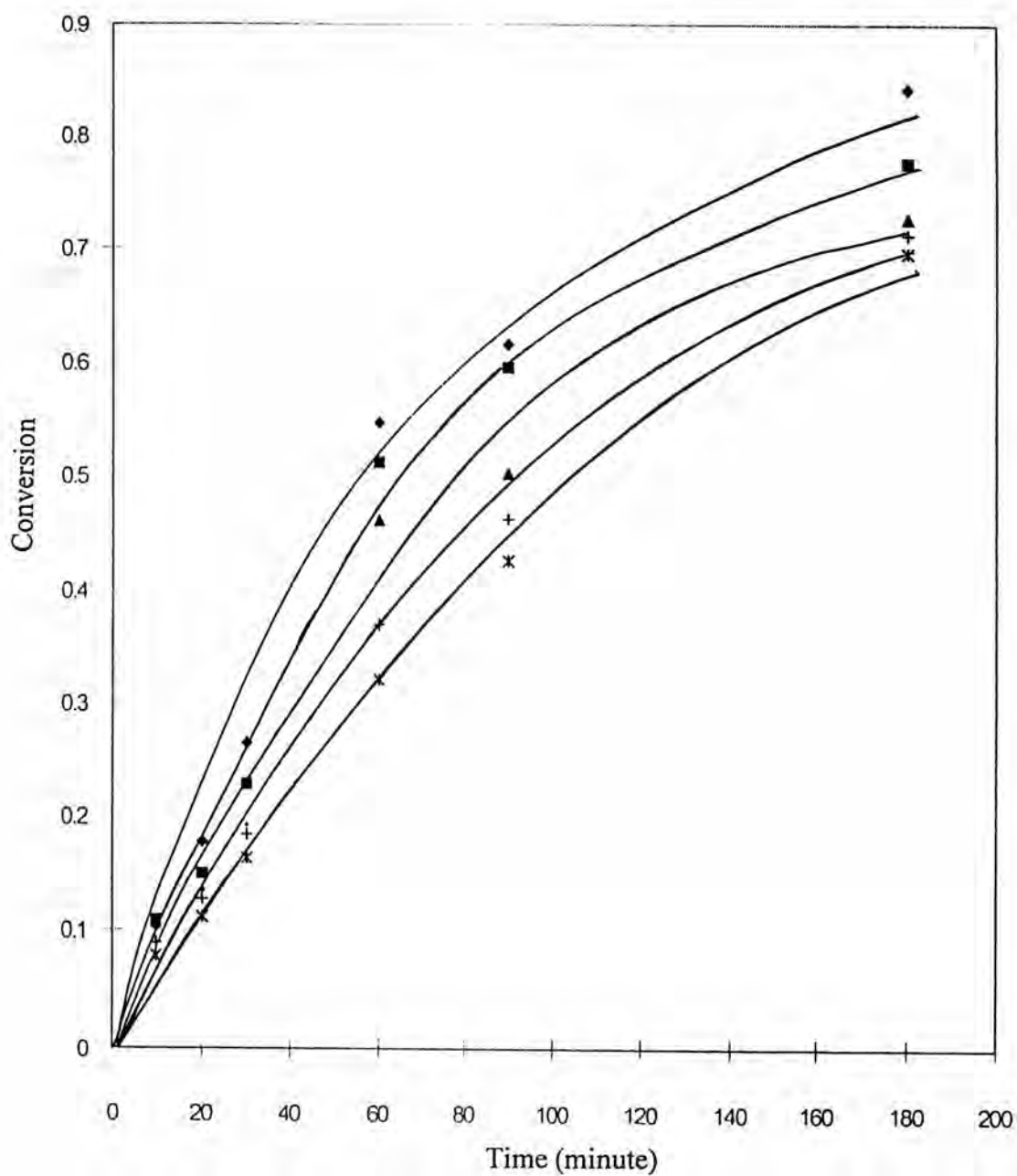
Figure 4.25 Plot of conversion versus time for LLDPE crosslinking at various
inhibitor concentrations at 446 K, 2.0% DCP; Irganox ◆, 0%; ■,0.10;
▲, 0.20%; +, 0.4%; *, 0.6%.(Rheometric technique)

Figure 4.26. Plot of conversion versus time for LDPE crosslinking at various inhibitor concentrations at 413 K, 2.0% DCP; Irganox ♦, 0%; ■,0.10; ▲, 0.20%; +, 0.4%; ✻, 0.6%.(DSC technique)
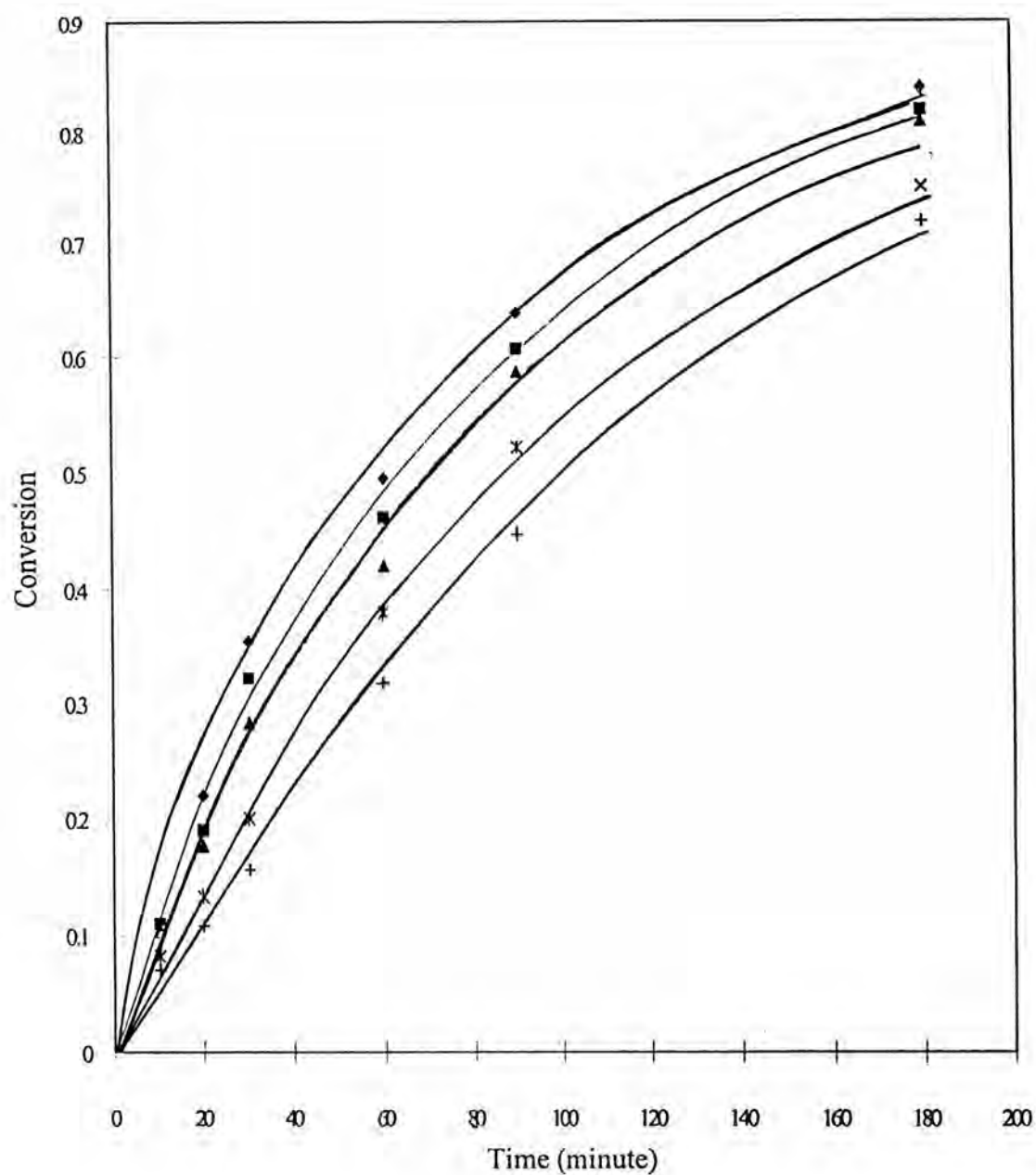
Figure 4.27. Plot of conversion versus time for LLDPE crosslinking at various inhibitor concentrations at 413 K, 2.0% DCP; Irganox ◆, 0%; ■,0.10; ▲, 0.20%; +, 0.4%; ✳, 0.6%.(DSC technique)

	Slope	Intercept	R-square
LDPE	-0.21	-5.47	0.950
LLDPE	-0.27	-6.06	0.910
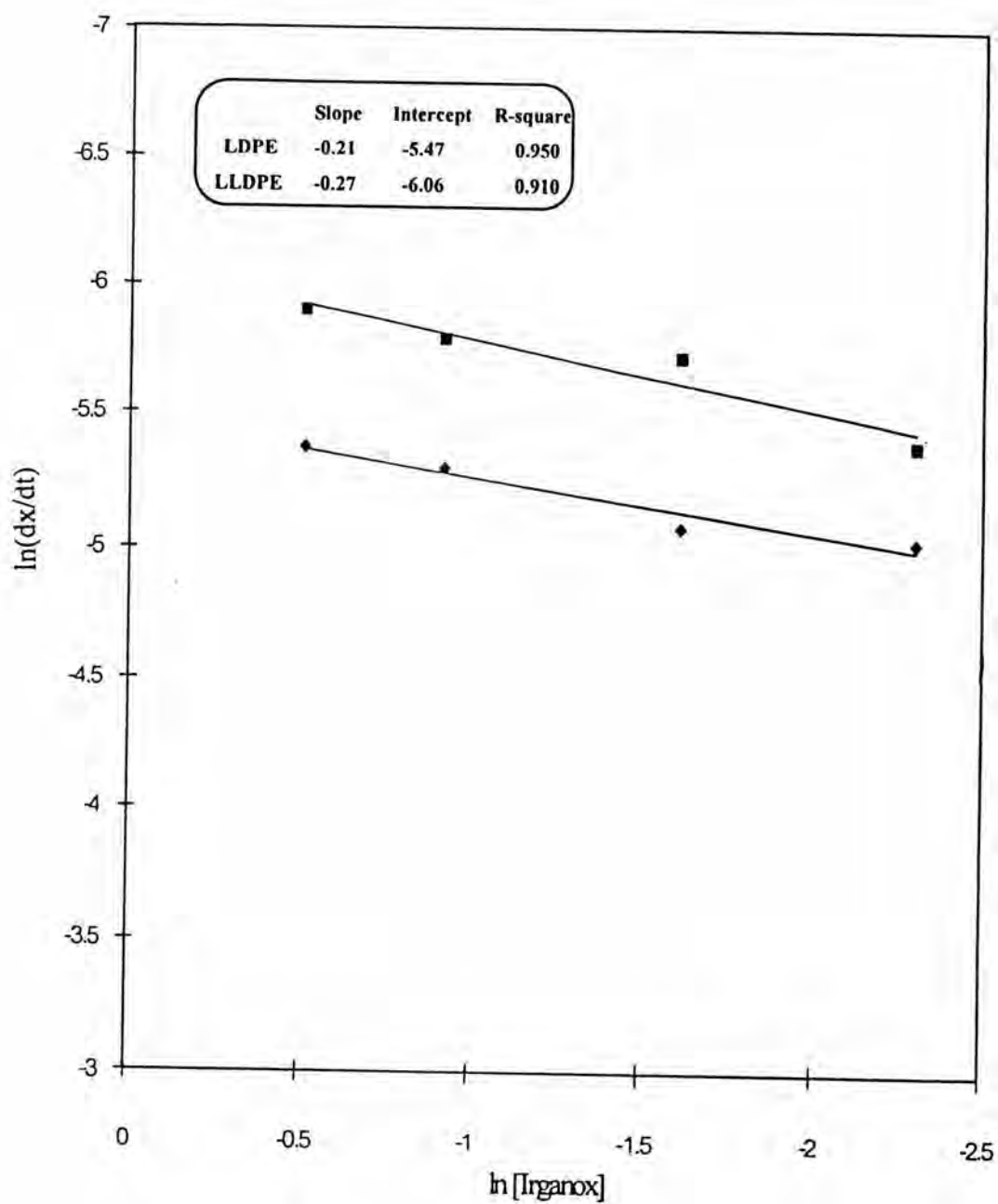
Figure 4.28 Plot of ln(dx/dt) versus ln[Irganox] at 446 K : ♦, LDPE; ■, LLDPE. (Rheometric technique).
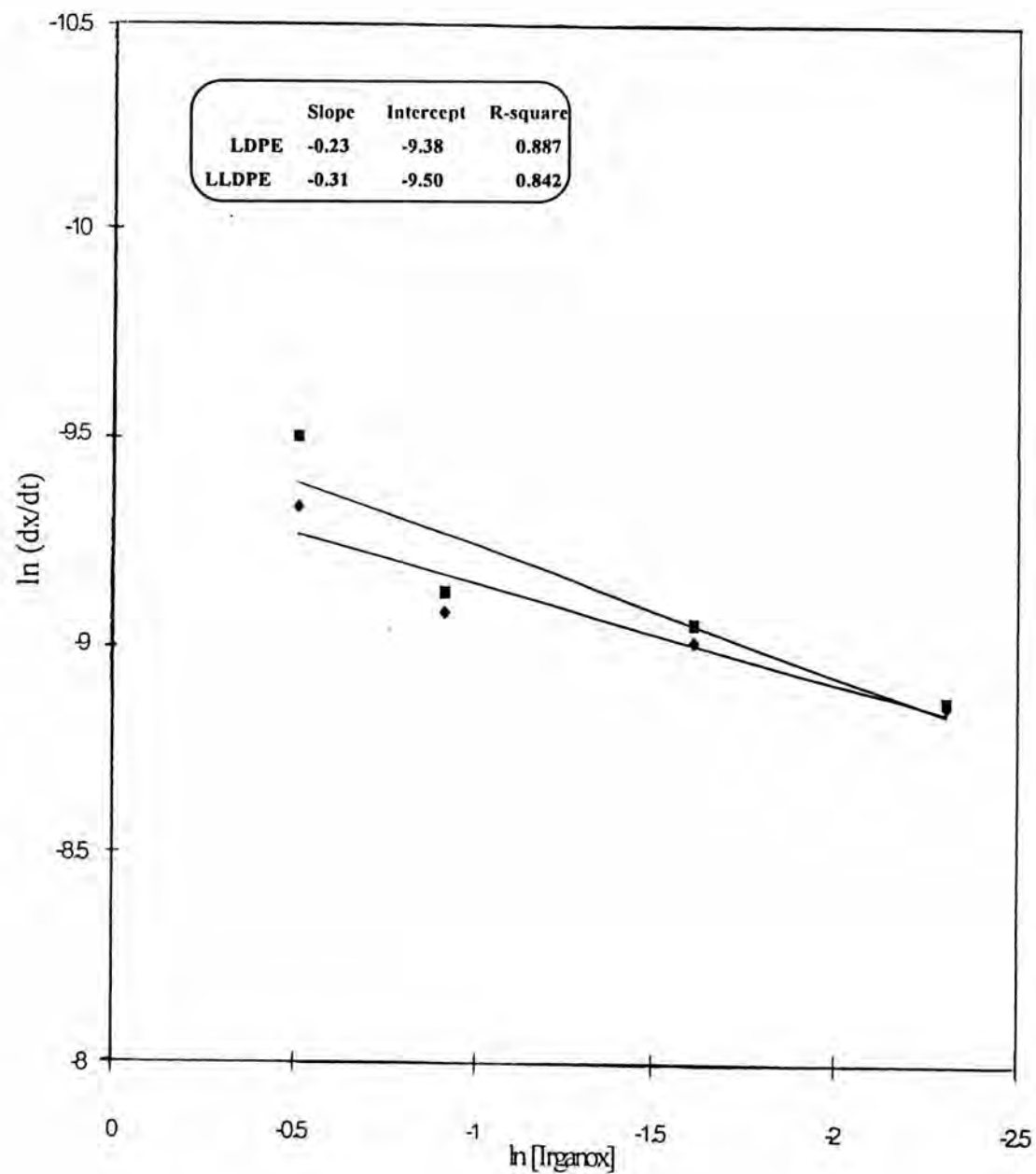
Figure 4.29 Plot of ln(dx/dt) versus ln[Irganox] at 413 K, DCP 2.0% : ◆, LDPE;
■, LLDPE.(DSC technique)

4.4 Effect of Initiator Concentration on Properties of the Crosslinked LDPE and LLDPE

4.4.1 Effect on Melting Temperature, Crystallization Temperature and Crystallinity

From Figures 4.30 and 4.31 and Table 4.4, T_m and crystallinity of the crosslinked LDPE and LLDPE decreased when DCP concentration increased, which has been found by P. J. Phillip and coworkers's [21-24].The loss of crystallinity was due to the less perfect crystals with increasingly distorted unit cell which increased as the crosslink density increased. Moreover, the lamellae thickness of the unit cells decreased, resulting in smaller crystals. Therefore, the size of crystallites of LDPE or LLDPE after crosslinking was smaller than those before. The smaller crystallites result in a decrease of the maximum melting temperature and caused the crosslinked LDPE and LLDPE more transparent than the uncrosslinking.

Table 4.6 The melting temperature (T_m), crystallization temperature (T_c), and crystallinity of LDPE and LLDPE after crosslinking.

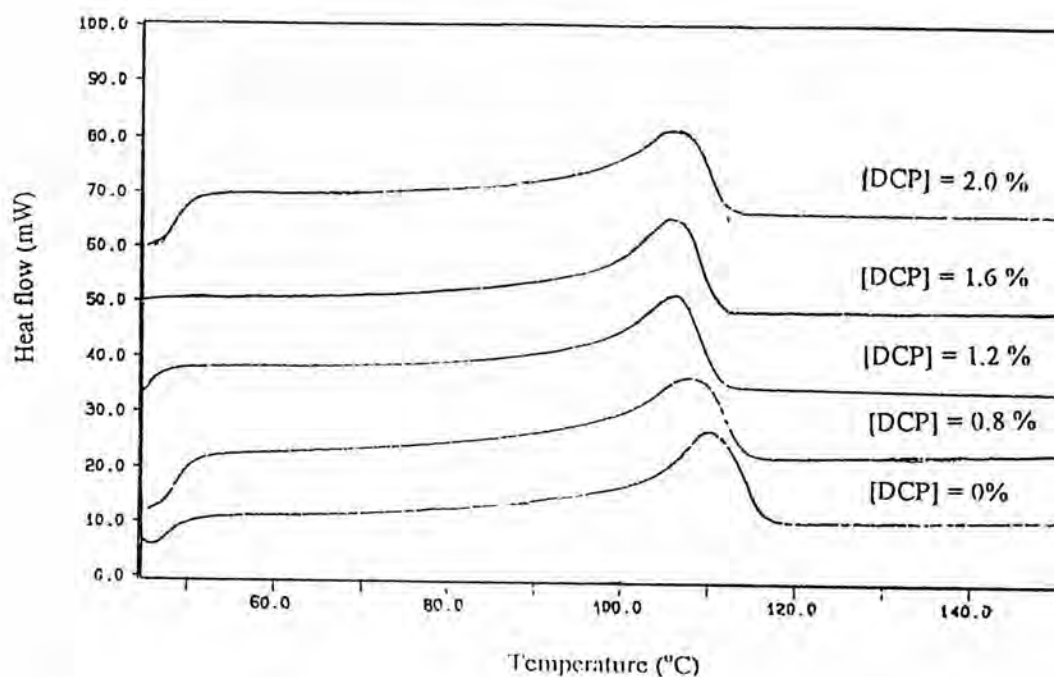| DCP	LDPE			LLDPE		
(%/w)	T_m ($^\circ$C)	T_c ($^\circ$C)	Crystallinity (%)	T_m ($^\circ$C)	T_c ($^\circ$C)	Crystallinity (%)
0	101.0	95.2	31.1	119.9	111.2	34.9
0.8	95.2	94.8	30.0	110.6	108.2	32.0
1.2	95.1	94.5	28.7	105.2	106.7	29.6
1.6	95.7	93.8	28.1	102.3	106.8	28.5
2.0	93.9	92.8	28.4	99.8	104.0	27.1

Figure 4.30 Melting temperature of LDPE after crosslinking at various DCP concentrations.
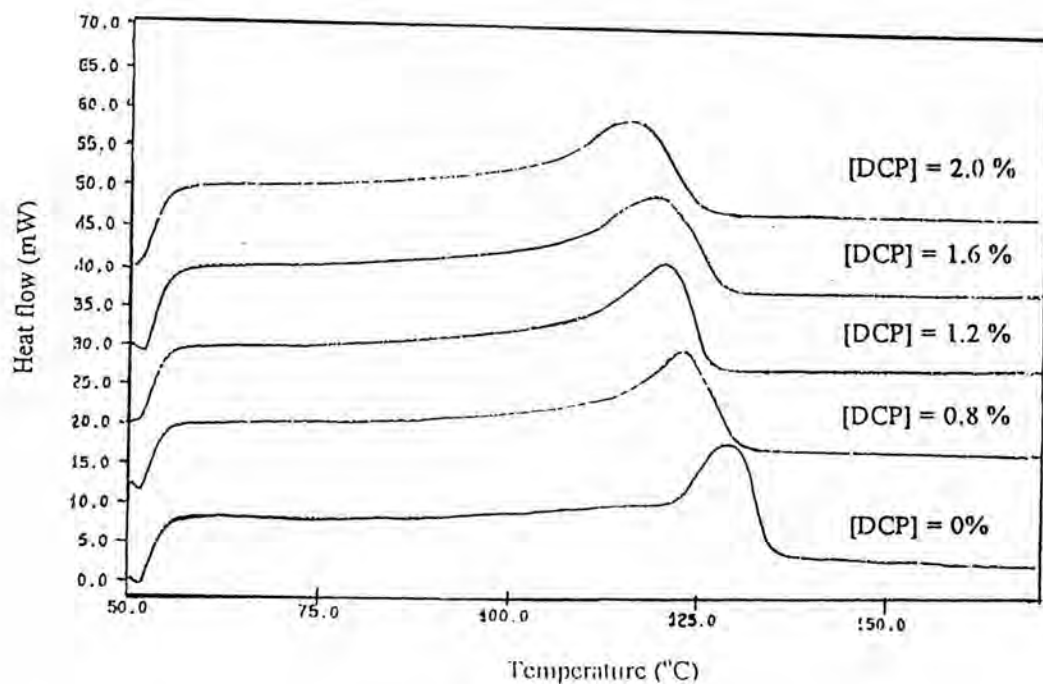

Figure 4.31 Melting temperature of LLDPE after crosslinking at various DCP concentrations.

4.4.2 Effect on Gel Content

It has been well-known that crosslinked polymers cannot be remelted and dissolved in any solvent but it is rather swell. Figure 4.32 shows that the gel content of the crosslinked LDPE and LLDPE increases with increasing DCP concentration from 0 upto 1.2%w/w and then trends to be constant. The excess peroxy radicals might react with the crosslinked polymer chains, leading to less probability to crystallization of polymer chain which resulted in the increase of crosslink density until reaching the constant of gel content at the high concentration of DCP. More than 1.6% of DCP for LDPE and LLDPE crosslinking was achieved a constant gel content of higher than 80 %.
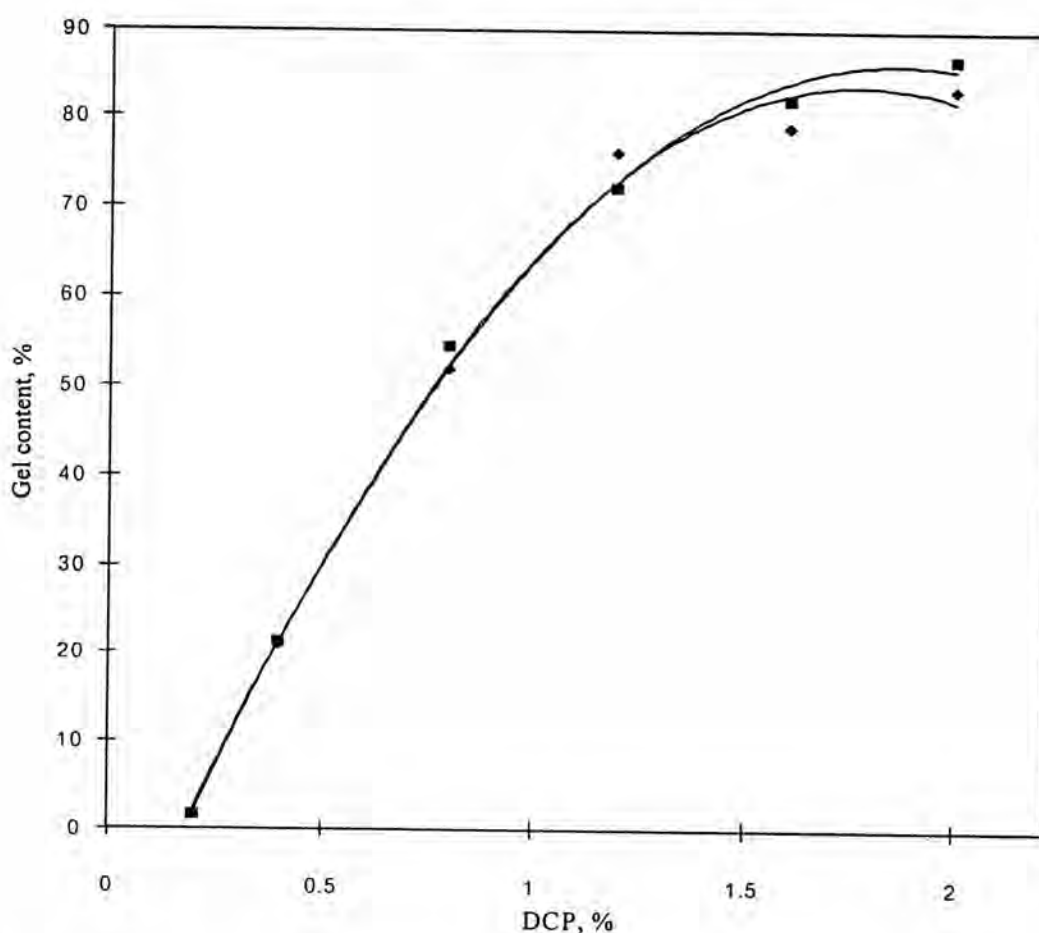

Figure 4.32 Effect of DCP concentration on the gel content of (♦) LDPE and
(■) LLDPE, cured at 180°C for 15 minutes.

4.5 Effect of Irganox 1010 on Gel Content

The gel content decreased with the increase of Irganox 1010 concentration (Figure 4.33) since the peroxy radicals were destroyed by the inhibitor. However, it seemed to be constant at the low inhibitor concentration due to the excess of DCP remained. The low concentration of Irganox 1010 (0.1-0.2%) did not significantly affect the gel content of the crosslinked LDPE and LLDPE with 2.0% DCP, but rather had the effect on the increase of crosslink density, which has not been proved here.
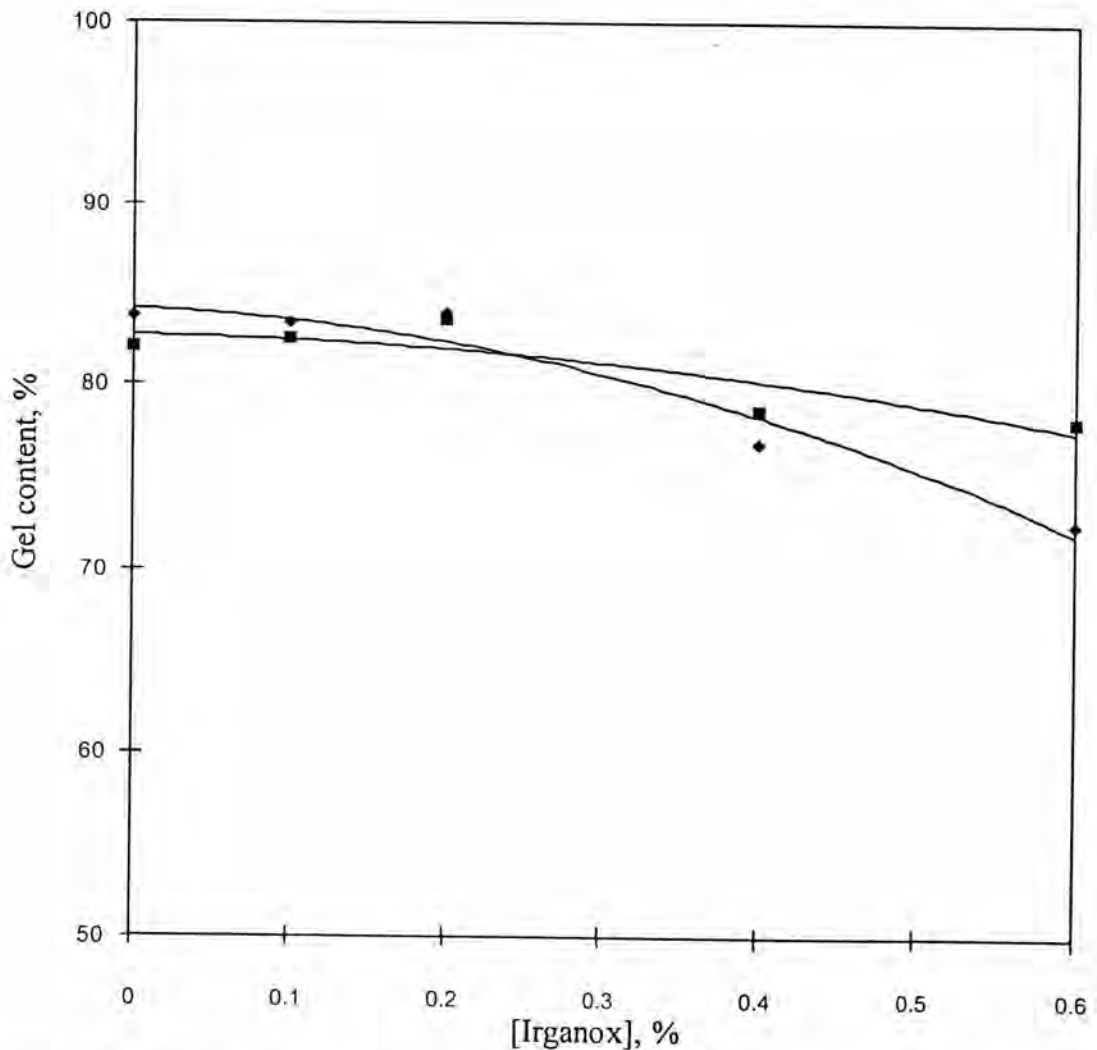

Figure 4.33 Effect of Irganox 1010 concentration on gel content (♦) LDPE and (■)LLDPE.